

AD-A104 852

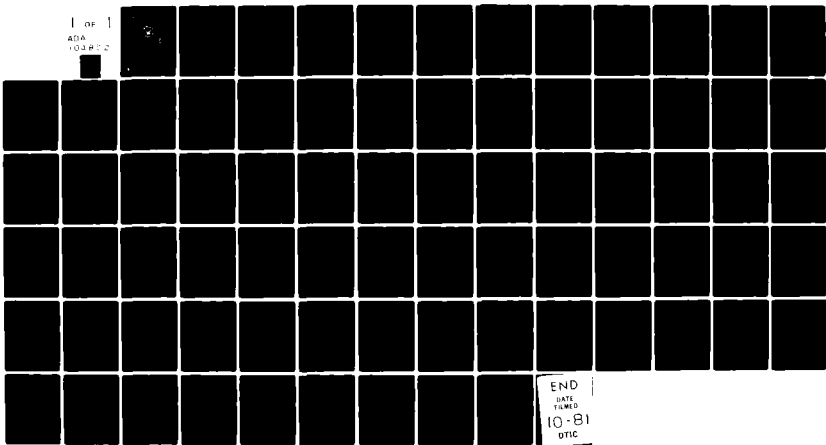
NAVAL POSTGRADUATE SCHOOL MONTEREY CA
ANALYSIS OF COMBUSTION OF A COMPOSITE PLATE. (U)
JUN 81 R E LUBY.

F/8 21/2

UNCLASSIFIED

NL

1 of 1
ADA
104852



END
DATE
FILMED
10-81
DTIC

AD A104852

NAVAL POSTGRADUATE SCHOOL
Monterey, California



DTIC
ELECTE
OCT 1 1981
S A D

THESIS

ANALYSIS OF COMBUSTION OF A COMPOSITE PLATE

by

Robert Emmett Luby, Jr.

June 1981

Thesis Advisor:

D. Salinas

Approved for public release; distribution unlimited

DTIC FILE COPY

81 10 047

Unclassified

SECURITY CLASSIFICATION OF THIS PAGE (When Data Entered)

REPORT DOCUMENTATION PAGE		READ INSTRUCTIONS BEFORE COMPLETING FORM
1. REPORT NUMBER	2. GOVT ACCESSION NO. AD-A104852	3. RECIPIENT'S CATALOG NUMBER
4. TITLE (and Subtitle) Analysis of Combustion of a Composite Plate.	5. TYPE OF REPORT & PERIOD COVERED Master's Thesis, June 1981	6. PERFORMING ORG. REPORT NUMBER
7. AUTHOR(s) Robert Emmett/Luby, Jr	8. CONTRACT OR GRANT NUMBER(s)	
9. PERFORMING ORGANIZATION NAME AND ADDRESS Naval Postgraduate School Monterey, California 93940	10. PROGRAM ELEMENT, PROJECT, TASK AREA & WORK UNIT NUMBERS	
11. CONTROLLING OFFICE NAME AND ADDRESS Naval Postgraduate School Monterey, California 93940	12. REPORT DATE June 1981	13. NUMBER OF PAGES 76
14. MONITORING AGENCY NAME & ADDRESS (if different from Controlling Office)	15. SECURITY CLASS. (of this report) Unclassified	15a. DECLASSIFICATION/DOWNGRADING SCHEDULE
16. DISTRIBUTION STATEMENT (of this Report) Approved for public release; distribution unlimited		
17. DISTRIBUTION STATEMENT (of the abstract entered in Block 20, if different from Report)		
18. SUPPLEMENTARY NOTES		
19. KEY WORDS (Continue on reverse side if necessary and identify by block number) Combustion, heat transfer, carbon, fiber, porous media		
20. ABSTRACT (Continue on reverse side if necessary and identify by block number) The combustion of a porous graphite fiber plate is analyzed. A transient one-dimensional, mathematical model is utilized to conduct numerous computer tests. The model simulates the thermal response of a porous graphite fiber plate and it is based on appropriate energy equations. Two of the energy equations are based on energy balances conducted on both the porous structure and on		

DD FORM 1473
1 JAN 73

EDITION OF 1 NOV 68 IS OBSOLETE
S/N 0102-014-6601

Unclassified
SECURITY CLASSIFICATION OF THIS PAGE (When Data Entered)

Unclassified

SECURITY CLASSIFICATION OF THIS PAGE/When Date Entered

Item #20 continued:

the air within the graphite fibers. The third energy equation is based on a mass balance performed on a differential volume of porous medium.

A test plan is formulated and computer test runs are conducted to investigate the effects of plate thickness, filament diameter, permeability, porosity and exterior wind velocity on the thermal response of the porous graphite fiber structure. The test results are analyzed and conclusions are presented.

A
series
for

Approved for public release; distribution unlimited

Analysis of Combustion of a Composite Plate

by

Robert Emmett Luby, Jr.
Lieutenant Commander, United States Navy
B.S., United States Naval Academy, 1973
M.E.M., Northwestern University, 1979

Submitted in partial fulfillment of the
requirements for the degree of

MASTER OF SCIENCE IN MECHANICAL ENGINEERING

from the

NAVAL POSTGRADUATE SCHOOL
June 1981

Author:

Robert E. Luby, Jr.

Approved by:

David Salinas

Thesis Advisor

Ray D. Deplante

Second Reader

P. J. Marts

Chairman, Department of Mechanical Engineering

William M. Tolles

Dean of Science and Engineering

ABSTRACT

The combustion of a porous graphite fiber plate is analyzed. A transient one-dimensional, mathematical model is utilized to conduct numerous computer tests. The model simulates the thermal response of a porous graphite fiber plate and it is based on appropriate energy equations. Two of the energy equations are based on energy balances conducted on both the porous structure and on the air within the graphite fibers. The third energy equation is based on a mass balance performed on a differential volume of porous medium.

A test plan is formulated and computer test runs are conducted to investigate the effects of plate thickness, filament diameter, permeability, porosity and exterior wind velocity on the thermal response of the porous graphite fiber structure. The test results are analyzed and conclusions are presented.

TABLE OF CONTENTS

I.	INTRODUCTION TO THE PROBLEM -----	8
II.	DESCRIPTION OF MATHEMATICAL MODEL -----	13
	A. AVERAGE PORE VELOCITY -----	13
	B. GOVERNING EQUATIONS -----	15
	C. BOUNDARY CONDITIONS -----	19
	D. ADDITIONAL ASSUMPTIONS -----	20
	E. METHOD OF NUMERICAL SOLUTION -----	20
III.	TEST PLAN FORMULATION -----	22
	A. EXTERIOR WIND VELOCITY (U_{∞}) -----	22
	B. PLATE THICKNESS (L) -----	22
	C. INTERNAL PLATE GEOMETRY -----	23
IV.	RESULTS AND OBSERVATIONS -----	26
	A. EFFECTS OF PLATE THICKNESS -----	29
	B. EFFECTS OF FILAMENT DIAMETER -----	34
	C. EFFECTS OF PERMEABILITY -----	38
	D. EFFECTS OF POROSITY -----	43
	1. Test Sets 21-24 ($p=.420$) -----	44
	2. Test Sets 17-20 ($p=.540$) -----	45
	3. Test Sets 25-28 ($p=.935$) -----	45
	E. EFFECTS OF EXTERIOR VELOCITY -----	46
V.	CONCLUDING REMARKS -----	49
	LIST OF REFERENCES -----	75
	INITIAL DISTRIBUTION LIST -----	76

LIST OF TABLES

TABLE I:	FIBER PROPERTIES -----	8
TABLE II:	TEST PLAN -----	25
TABLE III:	INITIAL CONDITIONS -----	28
TABLE IV:	COMPARISON OF TESTS SETS 1-4 WITH TEST SETS 13-16 -----	38
TABLE V:	OXYGEN DEPLETION LOCATIONS -----	39
TABLE VI:	PORE VELOCITY AND OXYGEN CONCENTRATION (TEST SETS 13-16) -----	41
TABLE VII:	PARAMETERS FOR TEST SETS 17-28 -----	44

LIST OF SYMBOLS

A^{-1}	- characteristic time of reaction
D	- ply thickness
d	- filament diameter
f	- stoichiometric ratio
h	- convection heat transfer coefficient
J	- Colburn j-factor
K	- thermal conductivity
L	- plate thickness
m	- specific permeability
\dot{m}	- mass flow rate
n	- number of nodal points
p	- porosity
R	- Universal Gas constant
r	- reaction rate
Re	- Reynolds number
s	- spacing between fibers
T	- temperature
t	- time
U_{∞}	- flow over exterior surface
u_p	- pore velocity

I. INTRODUCTION TO THE PROBLEM

The advent of advanced fiber-reinforced composite materials has spurred substantial research efforts across a broad spectrum. Whole organizations have been formed to analyze, design, and fabricate components made of composite materials.

Fibrous composites consist of long fibers contained within a matrix material. Long fibers are inherently much stiffer and stronger than the same material in bulk form. Fiber properties differ from those of the bulk form due to the more perfect structure of the fiber. Additionally, fewer internal defects are present in fibers than in bulk material. Strengths and stiffnesses of a few selected fiber material are presented in Table I below:

TABLE I: FIBER PROPERTIES

FIBER	DENSITY, ρ [lbm/in ³]	TENSILE STRENGTH, S [10 ³ lb/in ²]	S/ρ [10 ⁵ in]	TENSILE STIFFNESS, E [10 ⁴ lb/in ²]	E/ρ [10 ⁷ in]
Aluminum	.097	90	9	10.6	11
Titanium	.170	280	16	16.7	10
Steel	.282	600	21	30.0	11
Boron	.093	500	54	60.0	65
Graphite	.051	250	49	37.0	72

Boron and graphite fibers are frequently selected for composites that will be utilized as aircraft structural material.

The matrix material in such applications is frequently a plastic such as epoxy or polyimide. These advanced composites are characterized by properties that are superior to those of materials that have been previously utilized for aircraft structures (i.e. aluminum and titanium). Two major advantages are improved strength and stiffness, when compared with other materials on a unit weight basis.

Advanced composite materials have been designed that are three times as strong as aluminum, yet weigh only sixty percent as much [Ref. 1]. It is this favorable strength to weight ratio that makes composite materials particularly attractive to the aerospace industry.

Currently, almost every aerospace company is developing products made with fiber-reinforced composite materials. Replacement components are frequently made with composite materials. Examples of this application are the boron/epoxy fuselage section and horizontal tail on the General Dynamics F-111. Several companies are also introducing production components made from composite materials on their new aircraft. An example of this application is the F/A 18 Hornet Strike Fighter currently being built by McDonnell Douglas. The F/A 18 airframe is a balance of conventional materials and graphite epoxy composite. The wing skins, trailing edge flaps, stabilators, vertical tails and rudders, speed brake, and many access doors are made from composites. This balanced design has resulted in appreciable weight savings and increased aircraft performance.

Weight savings are of critical importance in military aircraft applications. Weight reductions result in the following desirable features:

- (1) Increased payload
- (2) Improved operating efficiency
- (3) Extended range

It is these attractive features that have created a great deal of interest within the U. S. Navy. Lighter weight aircraft with increased payload are ideal for carrier operations. Additionally, composite materials have improved the feasibility of VSTOL aircraft, which could lead to smaller, less expensive aircraft carriers.

The introduction of aircraft structural components made from composite materials and the potential of aircraft made entirely from composites has spurred a great deal of Navy sponsored research activity. Research is being conducted to gain insight into the following features of composite materials:

- (1) Thermal properties
- (2) Strength and stiffness
- (3) Fatigue life
- (4) Combustion characteristics

The combustion characteristics of composite materials and their thermal response in a fire environment are of particular concern to the Navy. The potential for aircraft carrier flight deck pool fires is quite high, due to the presence of various volatile fuels and ordnance on the flight deck during flight operations.

The response of metallic materials to aircraft carrier flight deck pool fires and the required fire-fighting techniques are well-known, but little data is available concerning the combustion characteristics of composite materials. In order to gain an insight into these characteristics an initial series of tests was conducted at the Naval Weapons Center, China Lake [Ref. 2]. The objective of these tests was to determine the response of graphite-epoxy composite materials to carrier flight deck pool fires and compare them with equivalent strength aluminum.

For these tests, a composite test specimen was mounted in such a manner as to simulate the heating condition of a complete wing subjected to a large pool fire. The various test specimens were then subjected to a steady state thermal environment. Specimen temperature data were recorded by thermocouple instrumentation until all internal reactions had ceased.

The combustion process was observed to proceed in two distinct phases:

- (1) Epoxy combustion
- (2) Graphite combustion

At the completion of the first stage, the epoxy was totally consumed, exposing the porous graphite fiber structure (epoxy ignites and burns at a much lower temperature than graphite). In some cases, the remaining graphite fibers exhibited characteristics of self-sustained combustion and a tendency to smolder, while in others the fibers would cool, indicating an inherent resistance to fire burn-through.

These initial tests indicated that the thermal response of a composite plate is not constant, but is a function of the various parameters that characterize the composite material (i.e. filament diameter, ply thickness, plate thickness), the exterior wind velocity, and the thermal environment. The number of parameters involved in the problem indicated that an exhaustive experimental program designed to further investigate the thermal response of a composite plate would not be economically feasible. Therefore, a computer model appeared to be a desirable means for conducting numerous tests.

II. DESCRIPTION OF MATHEMATICAL MODEL

In order to conduct a thorough computer analysis of the combustion characteristics of a graphite-epoxy composite plate, an appropriate mathematical model was required. A suitable one-dimensional model was previously formulated by Vatikiotis [Ref. 3]. The model was to simulate the thermal response, in one-dimension, of the graphite fiber mat after epoxy consumption. The following discussion summarizes the assumptions, governing equations, boundary conditions, and method of numerical solution utilized in the model.

A. AVERAGE PORE VELOCITY

In formulating the model it was assumed that an exterior wind velocity would always be present, thereby providing air flow over one surface of the composite plate. This assumption is quite realistic when one considers the relative wind velocities consistently present on aircraft carrier flight decks. The air flow produces a pressure differential across the composite plate. This pressure differential induces a convective air flow through the porous graphite structure governed by Darcy's Law,

$$u_p = \frac{-m}{\mu} \frac{dP}{dx} \quad (II.1)$$

where u_p is pore velocity, μ is the dynamic viscosity, dP/dx is the pressure gradient, and m is the specific permeability of the medium.

As a result of extensive experimental work, it has been suggested that Darcy's Law is valid only in those instances where $Re_i < 1$ [Ref. 4]. Therefore, internal Reynolds number was calculated in all test cases conducted. In all instances Re_i was on the order of 1 or less.

Pore velocity is a critical factor in the development of this mathematical model. This air flow enhances internal convection heat transfer, providing a means for extinction and eventual cooling of the graphite fibers. The air flow is also a source of oxygen for self-sustaining combustion, providing a means for heat generation within the porous structure. If the heat transfer, at a point, due to the air flow is greater than the heat generation, then cooling will occur at the point. If heat generation is greater than heat transfer at a point, then combustion will proceed at this location.

Equation (II.1) indicates that pore velocity (u_p) is a function of permeability (m). As a result of the critical relationship between pore velocity and thermal response, it was immediately assumed that permeability would be a critical factor in the formulation of the mathematical model.

Specific permeability is indicative of the ability of a porous medium to allow flow. It is dependent on geometry and on the properties of the medium itself. Several empirical models have been developed to obtain values for permeability. Vatikiotis selected a serial type representation proposed by Scheidegger [Ref. 5] in formulating this mathematical model:

$$m = \frac{1}{96} p(\delta/\tau)^2 \quad (\text{II.2})$$

where the porosity, p , is defined as,

$$p = 1 - \frac{\pi}{4} (d/D)^2 \quad (\text{II.3})$$

d is the filament diameter and D is the ply thickness (see Figure 1). The average pore diameter, δ , was calculated using an analogy to the hydraulic radius commonly utilized in fluids dynamics,

$$\delta = \frac{4D^2d}{\text{ARCTAN}(\theta)} \quad (\text{II.4})$$

The tortuosity, T , is a kinematical property equal to the average length of the flow path of a fluid particle from one side of a porous medium to the other. It is also a geometrical property dependent on the ratio d/D .

The above discussion indicates that the pore velocity utilized in the mathematical model is effected by the following parameters:

- (1) Plate thickness (D)
- (2) Filament diameter (d)
- (3) Permeability (m)
- (4) Porosity (p)
- (5) Exterior velocity (U_∞).

B. GOVERNING EQUATIONS

After an expression for average pore velocity had been derived, appropriate energy equations were developed.

Vatikiotis [Ref. 3] performed energy balances on both the

porous solid and on the air within the graphite fiber structure in order to develop the proper equations. The energy balances utilized the control volume approach. This approach is summarized as follows:

$$\text{Heat into } \frac{dv}{dv} + \text{Heat Generation within } dv = \text{Heat out of } dv + \text{Increase in Internal Energy}$$

where $dv = dx dy dz$.

By utilizing the porous medium as a control volume, the fiber heat transfer equation was formulated. Conduction, convection, radiation, change in internal energy, and heat generation rate per unit volume were all considered in the formulation of this equation.

In developing the fiber heat transfer equation, Vatikiotis [Ref. 3] limited the model to the kinetic regime of combustion and assumed that the dominant chemical reaction was



This idealized treatment of the actual reaction is a good approximation during the initial combustion of the graphite fibers.

An internal flow heat transfer equation was obtained by performing an energy balance on a differential volume of air. Heat conduction through the air, convection from the fibers to the air, and energy transport due to air flow were all considered in the formulation of this equation.

In developing the internal flow heat transfer equation, Vatikiotis [Ref. 3] utilized the perfect gas assumption for air in order to calculate enthalpy as follows:

$$dh = C_a dT_a \quad (II.5)$$

where C_a is the specific heat of air at constant pressure.

The effects of the combustion by-products on air were assumed to be negligible allowing the mass flow to be represented as,

$$\dot{m}_a = \rho_a \omega u_p dydz \quad (II.6)$$

Equations II.5 and II.6 were then utilized to determine the energy transport due to the air flow, $\dot{m}_a h$.

In both the fiber heat transfer equation and the internal flow heat transfer equation, thermal conduction was determined by Fourier's Law of heat conduction in the following form:

$$q_{\text{cond}} = -K \frac{T}{x} dydz \quad (II.7)$$

Similarly, convection heat transfer was determined in both equations by application of the following expression:

$$q_{\text{conv}} = h_i (T_g - T_a) dA \quad (II.8)$$

where T_g is the temperature of the graphite, T_a is the temperature of the air, dA is the surface area of the graphite in the differential volume, and h_i is the internal convection heat transfer coefficient. An empirical expression developed by Yoshida, Ramaswami, and Hougen [Ref. 6] was used to determine h_i .

The final field equation formed was the oxygen transport equation. In order to formulate this equation a mass balance was performed on a differential volume of porous medium. The mass balance was formulated in the following manner:

Oxygen into $\frac{dv}{dv}$ = Oxygen out $\frac{of}{dv}$ + Oxygen Consumption + Oxygen Accumulation

Two mass transport mechanisms were considered in formulating this equation:

(1) \dot{m}_B - molecular diffusion

(2) \dot{m}_C - convective transport due to mass flow

Molecular diffusion was determined by Fick's Law,

$$\dot{m}_B = B \frac{\partial \phi}{\partial x} dydz \quad (II.9)$$

where B is the diffusivity of oxygen into the porous medium.

The convective transport term was determined by

$$\dot{m}_C = \rho u_p \phi dydz \quad (II.10)$$

Oxygen consumption rate was determined by multiplying reaction rate, $r(T_g, \phi)$, by the stoichiometric ratio (1/f) of the reaction. The reaction rate is of the Arrhenius type,

$$r = A(T, \phi) \exp(-E/RT)$$

where A^{-1} is the characteristic time of the chemical reaction, E is the activation energy, R is the universal gas constant, T is absolute temperature and ϕ is the concentration of oxygen. The reaction rate was determined by utilizing an empirical expression developed by Frank-Kamenetski [Ref. 7].

The three field equations described above are presented below:

(1) Fiber Heat Transfer Equation

$$\frac{\partial}{\partial x} [(K_g + K_r) \frac{\partial T_g}{\partial x}] - \frac{h_i^2}{(1-p)} (T_g - T_a) + \Delta H r(T_g, \phi) = \rho_g C_g \frac{\partial T_g}{\partial t} \quad (II.11)$$

(2) Internal Flow Heat Transfer Equation

$$\frac{\partial}{\partial x} \left[\left(K_a \frac{\partial T_a}{\partial x} \right) - \dot{m} c_a \frac{\partial T_a}{\partial x} + \frac{h i z}{p} (T_g - T_a) \right] = \rho_a c_a \frac{\partial T_a}{\partial t} \quad (\text{II.12})$$

(3) Oxygen Transport Equation

$$\frac{\partial}{\partial x} \left(B \frac{\partial \phi}{\partial x} \right) - u_p \frac{\partial \phi}{\partial x} - \frac{\partial u_p}{\partial T_a} \left(\frac{\partial T_a}{\partial x} \right) \phi - \left(\frac{1}{f} \right) r(T_g, \phi) = \frac{\partial \phi}{\partial t} \quad (\text{II.13})$$

Several of the parameters included in equations II.11, II.12, and II.13 are functions of temperature (i.e. thermal conductivity, reaction rate). This temperature dependence was retained in the mathematical model and the parameters were changed with temperature.

C. BOUNDARY CONDITIONS

In order to make the mathematical model results as meaningful as possible, it was desired that boundary conditions be imposed that simulated the experiments of Fontenot [Ref. 1]. Vatikiotis imposed the following boundary conditions:

$$(K_g + K_r) \frac{\partial T_g}{\partial x} = h_1 (T_g - T_\infty) + \sigma \epsilon (T_g^4 - T_\infty^4) \text{ at } x = 0 \quad (\text{II.14})$$

$$(K_g + K_r) \frac{\partial T_g}{\partial x} = -h_2 (T_g - T_\infty) - \sigma \epsilon (T_g^4 - T_\infty^4) \text{ at } x = L \quad (\text{II.15})$$

$$T_a = T_\infty \text{ at } x = 0 \quad (\text{II.16})$$

$$\frac{\partial T_a}{\partial x} = \frac{\partial T_g}{\partial x} \text{ at } x = L \quad (\text{II.17})$$

$$B \frac{\partial \phi}{\partial x} = u_p (\phi - \rho \phi_\infty) \text{ at } x = 0 \quad (\text{II.18})$$

$$\frac{\partial \phi}{\partial x} = 0 \text{ at } x = L \quad (\text{II.19})$$

The above boundary conditions provide a reasonable model for the one-dimensional problem. Boundary conditions II.14 and II.15 consider convection and radiation heat transfer from the porous graphite structure. Boundary condition II.16 sets the air entering the porous plate at ambient temperature. Boundary conditions II.18 and II.19 are Dankwert conditions [Ref. 8] for flow through a porous media.

D. ADDITIONAL ASSUMPTIONS

The mathematical model is further based on two additional assumptions not previously described.

(1) The temperature across each individual fiber is assumed to be constant. This assumption is quite reasonable due to the small diameter of the graphite fibers.

(2) The temperature of the air in each individual pore is assumed to be constant.

These two assumptions should not be interpreted as limiting the temperature from fiber to fiber, or from pore to pore. The model allows temperatures to vary according to the equations described above.

E. METHOD OF NUMERICAL SOLUTION

The field equations form a system of three nonlinear, coupled partial differential equations. A Galerkin formulation of the finite element method is utilized to obtain solutions of the field equations. Linear interpolation functions are used as the basis functions.

The plate thickness (L) is considered to form a closed domain $(0, L)$ that is partitioned into $(n-1)$ elements. This process results in an n nodal point model. In accordance with the Galerkin method, a system of ordinary differential equations is finally obtained.

The resulting system contains $3n$ ordinary differential equations (graphite temperature, air temperature, and oxygen concentration at each nodal point). These equations retain the character of the original set of partial differential equations.

Initial tests were conducted using a 21 nodal point model (63 o.d.e.). Several instances of numerical instability were discovered for twenty one nodal point computer runs. Thirty-one nodal point and thirty-five nodal point models were tested, with convergence obtained within five percent. A thirty-one nodal point model (93 o.d.e.) was selected for all subsequent test runs.

III. TEST PLAN FORMULATION

It was desired that the thermal response of a composite plate be thoroughly analyzed. In order to carry out this objective, a test plan was formulated for use with the one-dimensional combustion model described in Section II. Initial efforts in formulating the test plan concerned selection of input parameters for variation during testing.

A. EXTERIOR WIND VELOCITY (U_{∞})

Exterior air flow rate (U_{∞}) was immediately selected as a test parameter because of its obvious effects on average pore velocity and because it acts as a source of oxygen for the combustion process. It was felt that relative wind velocities between ten and ninety knots would be representative of the velocities commonly experienced on aircraft carrier flight decks. Wind velocities of 10, 40, 70, and 90 knots were selected for testing.

B. PLATE THICKNESS (L)

Plate thickness (L) is a critical parameter because it also effects pore velocity. A consideration of Darcy's Law points out the effects of plate thickness on pore velocity,

$$u_p = \frac{m}{\mu} \frac{\Delta p}{L} \quad \text{(III.1)}$$

where Δp is the pressure differential across the plate, m is the specific permeability of the medium, and μ is the dynamic

viscosity. As can be seen in equation III.1, pore velocity (u_p) decreases hyperbolically as plate thickness increases. The effect of plate thickness on pore velocity was felt to be quite relevant because it could produce extremely high or extremely low pore velocities, both of which could result in extinction. Plate thicknesses of 1.0 inch, 0.5 inch, 0.25 inch, and 0.125 inch were selected for testing. It was felt that these thicknesses were typical of composite plates under consideration for use as airframe material.

C. INTERNAL PLATE GEOMETRY

The pore velocity equation (II.1) indicated that both permeability and porosity of the porous medium were significant factors in analyzing the thermal response of the composite plate. Porosity is a measure of void space and is indicative of the space available for oxygen, while permeability represents the ability of a porous medium to allow flow. Equations II.2 and II.3 indicated that filament diameter (d) and ply thickness (D) significantly effect both porosity and permeability (see Figure 1). Filament diameters of .0002 inch, .0004 inch, .002 inch, and .004 inch were selected for testing. Ply thicknesses of .0005 inch and .005 inch were utilized in the testing program. These selections of filament diameter (d) and ply thickness (D) allowed for consideration not only of the effects of fiber diameter, porosity, and permeability, but also the effects of changing permeability while holding porosity constant.

It was also desired to consider the effects of changing porosity while holding permeability constant. In order to accomplish this objective, specific filament diameters and ply thicknesses were selected such that permeability remained the same in each case. The following selections accomplished this task:

1. $d = .003$ inch; $D = .004$ inch
2. $d = .006$ inch; $D = .007$ inch
3. $d = .0002$ inch; $D = .0007$ inch

The final test plan is presented as Table II. This (4 x 28) matrix of computer runs resulted in production of 112 different cases for analysis. In addition to graphite temperature (T_g), air temperature (T_a), and oxygen concentration, the following system parameters were calculated as functions of time and position for each case:

- (1) Filament diameter
- (2) Porosity
- (3) Permeability
- (4) Pore velocity
- (5) Internal Reynolds number
- (6) Internal heat transfer coefficient
- (7) Reaction rate
- (8) Filament conductivity
- (9) Diffusion coefficient of oxygen

Therefore, each of the computer runs produced data concerning changes in temperature and oxygen concentration and changes in system parameters.

TABLE II: TEST PLAN

SET	PLATE THICKNESS [IN]	FILAMENT DIAMETER [IN]	PLY THICKNESS [IN]	CASE A [KNOTS]	CASE B [KNOTS]	CASE C [KNOTS]	CASE D [KNOTS]
1	0.5	.004	.005	U ₈ =90	U ₈ =70	U ₈ =40	U ₈ =10
2	1.0	.004	.005	U ₈ =90	U ₈ =70	U ₈ =40	U ₈ =10
3	0.25	.004	.005	U ₈ =90	U ₈ =70	U ₈ =40	U ₈ =10
4	0.125	.004	.005	U ₈ =90	U ₈ =70	U ₈ =40	U ₈ =10
5	0.5	.002	.005	U ₈ =90	U ₈ =70	U ₈ =40	U ₈ =10
6	1.0	.002	.005	U ₈ =90	U ₈ =70	U ₈ =40	U ₈ =10
7	0.25	.002	.005	U ₈ =90	U ₈ =70	U ₈ =40	U ₈ =10
8	0.125	.002	.005	U ₈ =90	U ₈ =70	U ₈ =40	U ₈ =10
9	0.5	.0002	.0005	U ₈ =90	U ₈ =70	U ₈ =40	U ₈ =10
10	1.0	.0002	.0005	U ₈ =90	U ₈ =70	U ₈ =40	U ₈ =10
11	0.25	.0002	.0005	U ₈ =90	U ₈ =70	U ₈ =40	U ₈ =10
12	0.125	.0002	.0005	U ₈ =90	U ₈ =70	U ₈ =40	U ₈ =10
13	0.5	.0004	.0005	U ₈ =90	U ₈ =70	U ₈ =40	U ₈ =10
14	1.0	.0004	.0005	U ₈ =90	U ₈ =70	U ₈ =40	U ₈ =10
15	0.25	.0004	.0005	U ₈ =90	U ₈ =70	U ₈ =40	U ₈ =10
16	0.125	.0004	.0005	U ₈ =90	U ₈ =70	U ₈ =40	U ₈ =10
17	0.5	.003	.004	U ₈ =90	U ₈ =70	U ₈ =40	U ₈ =10
18	1.0	.003	.004	U ₈ =90	U ₈ =70	U ₈ =40	U ₈ =10
19	0.25	.003	.004	U ₈ =90	U ₈ =70	U ₈ =40	U ₈ =10
20	0.125	.003	.004	U ₈ =90	U ₈ =70	U ₈ =40	U ₈ =10
21	0.5	.006	.007	U ₈ =90	U ₈ =70	U ₈ =40	U ₈ =10
22	1.0	.006	.007	U ₈ =90	U ₈ =70	U ₈ =40	U ₈ =10
23	0.25	.006	.007	U ₈ =90	U ₈ =70	U ₈ =40	U ₈ =10
24	0.125	.006	.007	U ₈ =90	U ₈ =70	U ₈ =40	U ₈ =10
25	0.5	.0002	.0007	U ₈ =90	U ₈ =70	U ₈ =40	U ₈ =10
26	1.0	.0002	.0007	U ₈ =90	U ₈ =70	U ₈ =40	U ₈ =10
27	0.25	.0002	.0007	U ₈ =90	U ₈ =70	U ₈ =40	U ₈ =10
28	0.125	.0002	.0007	U ₈ =90	U ₈ =70	U ₈ =40	U ₈ =10

IV. RESULTS AND OBSERVATIONS

In analyzing each computer run, particular attention was directed at the combustion-extinction phenomenon. Initial output indicated that a particular combustion flash point did not exist for prescribed initial conditions. Instead, it was surmised that a combustion continuum exists for a composite plate, ranging from immediate extinction, to immediate total plate combustion. This conjecture resulted in an additional research objective of attempting to determine the nature of this continuum. Placement of the different computer runs in the speculated combustion continuum was a necessarily subjective process. The following general categories were utilized:

- (1) Immediate extinction
- (2) Slight combustion, fast cooling
- (3) Slight combustion, slow cooling
- (4) Moderate combustion
- (5) Extensive combustion
- (6) Rapid combustion

The effect of each of the input parameters on the combustion-extinction process was studied extensively. It was expected that by analyzing these effects for numerous computer runs, that the combustion continuum for a particular plate and prescribed initial conditions would be understood, and that the effects of system parameters would be discovered. This

information could then be utilized to select those design parameters that improve the flame resistance of composite materials. Improved flame resistance would increase the survivability of a composite structure.

A graphics package was inserted in the program to allow for ease of interpretation of results. Graphite temperature, air temperature, oxygen concentration, reaction rate, and the various system parameters listed above were all included in the plotting procedure. The plots are presented as functions of plate location for particular times.

The initial conditions prescribed for the 112 computer runs are presented in Table III.

An initial graphite temperature of 1050°F was selected as a result of several preliminary test runs. These test runs indicated an ignition temperature in the vicinity of 1050°F for filament diameters (d) and ply thicknesses (D) of the same order of magnitude as those called for by the test plan.

Initial air temperatures were selected to simulate a steady increase in temperature from ambient (50°F) at the entrance to 1050°F in the plate interior.

It was observed that initial oxygen concentration had little effect on the solution. The mathematical model immediately settled on the oxygen concentration appropriate for the particular test case, no matter which initial oxygen concentration was utilized.

TABLE III: INITIAL CONDITIONS

NODAL POINT	X/L	GRAPHITE TEMPERATURE	AIR TEMPERATURE	OXYGEN CONCENTRATION
		[°F]	[°F]	[lbm/FT ³]
1	0.0	1050.0	50.0	.004
2	0.03333	1050.0	150.0	.004
3	0.06667	1050.0	250.0	.004
4	0.10000	1050.0	350.0	.004
5	0.13333	1050.0	450.0	.004
6	0.16667	1050.0	550.0	.004
7	0.20000	1050.0	650.0	.004
8	0.23333	1050.0	750.0	.004
9	0.26667	1050.0	850.0	.004
10	0.30000	1050.0	950.0	.004
11	0.33333	1050.0	1050.0	.004
12	0.36667	1050.0	1050.0	.004
13	0.40000	1050.0	1050.0	.004
14	0.43333	1050.0	1050.0	.004
15	0.46667	1050.0	1050.0	.004
16	0.50000	1050.0	1050.0	.004
17	0.53333	1050.0	1050.0	.004
18	0.56667	1050.0	1050.0	.004
19	0.60000	1050.0	1050.0	.004
20	0.63333	1050.0	1050.0	.004
21	0.66667	1050.0	1050.0	.004
22	0.70000	1050.0	1050.0	.004
23	0.73333	1050.0	1050.0	.004
24	0.76667	1050.0	1050.0	.004
25	0.80000	1050.0	1050.0	.004
26	0.83333	1050.0	1050.0	.004
27	0.86667	1050.0	1050.0	.004
28	0.90000	1050.0	1050.0	.004
29	0.93333	1050.0	1050.0	.004
30	0.96667	1050.0	1050.0	.004
31	1.0000	1050.0	1050.0	.004

These initial conditions produced results that ranged from immediate extinction to moderate combustion for the 112 test runs. The influence of the input parameters on the combustion-extinction phenomenon was quite pronounced in several cases, these effects will now be considered.

A. EFFECTS OF PLATE THICKNESS

The test plan provided four plate thicknesses in order to explore the effects of this parameter on thermal response.

The thicknesses were as follows:

- (1) 0.125 inch
- (2) 0.250 inch
- (3) 0.500 inch
- (4) 1.000 inch

It was generally observed that varying plate thickness produced two extinction regions, existing on both sides of a combustion region. Slight to extensive combustion was observed for the test runs when in the combustion region. The two extinction regions are the result of two different phenomena:

- (1) 'Choking' of oxygen flow - pore velocity and oxygen concentration are depleted to such an extent that combustion cannot be supported;
- (2) 'Blowout' - oxygen concentration and pore velocity are of such magnitude that convective heat transfer overcomes heat generation and cooling occurs.

As a specific example of plate thickness effects consider test sets 1-4. The following parameters characterized the plate geometry for these test sets:

- (1) Filament diameter = .004 inch
- (2) Ply thickness = .005 inch

The .125 inch plates (test set 4) experienced extinction for all exterior velocities. Figure 2 depicts the extinction process for the 0.125 inch plate, with an exterior wind velocity of 90 knots. Graphite temperatures are decreasing at all locations and oxygen concentration is high at all locations, ranging from .007-.008 lbm/FT³. These thin plates are characterized by high pore velocities, typically greater than 10,000 FT/HR. (see Figure 5). These high pore velocities and oxygen concentrations indicate that extinction occurs as a result of the 'blowout' phenomenon. The high pore velocities enhance convective heat transfer producing the cooling effect depicted in Figure 2. The high pore velocities were expected for the thin plates because pore velocity is governed by Darcy's Law. As previously pointed out, pore velocity increases hyperbolically as plate thickness decreases.

The .25 inch plates (test set 3) experienced moderate combustion for all velocities tested, with the exception of ten knots. Figure 4, 5, and 6 depict a typical combustion sequence for plates of this thickness. As these figures indicate, the combustion process initiates in a region removed from the plate entrance, eventually moving to the surface of the plate. It appears that some initial cooling of the graphite fibers is occurring in the plate entrance regions. The

situation is only temporary though, until self-sustaining combustion initiates in the plate interior. The oxygen supply follows the combustion sequence with all oxygen being consumed in the combustion region and zero oxygen concentration existing beyond this region (see Figure 7). The oxygen concentration results explain the movement of the combustion region from the plate interior to the plate surface. The combustion process is utilizing all the available oxygen in order to sustain itself, but additional oxygen could be used to enhance combustion. Therefore, the combustion region moves toward the entrance, where the most abundant oxygen supply exists.

Pore velocities for the 0.250 inch plates are greatly reduced from those of the previously discussed thinner plates. Velocities of 7000 FT/HR are typical. The increased thickness reduced the pore velocity to such an extent that convecting heat transfer is no longer removing heat at a rate great enough to provide cooling, but the velocity is of sufficient magnitude to provide enough oxygen to support moderate combustion in the later half of the plate. It is thought that combustion initiates in the plate interior and not on the plate surface because pore velocity is high enough to provide some initial cooling at the plate entrance. It is further thought that continued reductions in pore velocity would result in reduction of the cooled entrance region. A critical pore velocity could be reached where no entrance cooling is achieved, but the velocity is sufficient to support combustion throughout the entire

plate. Pore velocity reductions beyond this critical point would result in insufficient oxygen supply to support combustion throughout the entire plate. Combustion initiation in the front half of the plate would characterize this situation. The results obtained from the .5 inch plates appear to support this speculation.

The .5 inch plates (test set 1) experienced moderate combustion similar to the .25 inch plates for all velocities tested, with the exception of ten knots. The combustion process for these plates differed from that of the .25 inch plates in the location of the combustion initiation region. As can be seen in Figure 8, combustion initiates in the plate entrance region. Pore velocities of 3500 FT/HR were typical for these plates. It appears that the reduction in pore velocity greatly reduced the cooling effect in the plate entrance regions noted in the .25 inch plates, but that the velocity was still high enough to support combustion in this region.

The 1.0 inch plates (test set 2) experienced slight local combustion in the plate entrance region, with eventual extinction occurring for all velocities tested. In all cases, pore velocities were not sufficient to support combustion for an extended period of time. As can be seen in Figure 9, oxygen concentration is rapidly falling even with an exterior wind velocity of ninety knots. This lack of oxygen within the plate interior effectively chokes the combustion process resulting in extinction at all velocities tested.

The effects of thickness on thermal response are quite evident from the above tests. Thin plates are desirable in that extinction by 'blowout' is frequently achieved, but thin plates are still susceptible to combustion if average pore velocity is reduced to such an extent that the thermal response moves from the 'blowout' region to the combustion region. Reduced exterior wind velocity, or a change in internal plate geometry that results in reduced permeability could both move the thermal response for a thin plate to the combustion region.

Thick plates are advantageous in that extremely low pore velocities are frequently achieved. This situation results in a 'choking' of oxygen flow that will lead to extinction. The choking phenomena is not particularly desirable in that the plate interior does not cool as rapidly as when extinction occurs by 'blowout'. High temperatures remain in the center of the plate for long periods of time. This type of situation probably occurred when 'smoldering' was observed in several of the tests conducted by Fontenot [Ref. 2].

Thick plates are also susceptible to combustion if high exterior velocities occur or if plate geometry is altered so that permeability is increased.

In analyzing the tests for various thicknesses, a good deal was learned about combustion initiation. It was learned that the initiation region is controlled by pore velocity, which is influenced by plate thickness. It was also learned that the size of the combustion initiation region is quite

sensitive to pore velocity, with a critical velocity existing for a particular plate geometry, such that the entire plate will experience combustion if this velocity is present.

B. EFFECTS OF FILAMENT DIAMETER

Altering fiber diameter, while holding all other system parameters constant, again results in the three characteristic thermal response regions previously described (choking - combustion-blowout). Varying only fiber diameter results in a change in the internal geometry of the plate. A decrease in fiber diameter (d) will effect an increase in both porosity and permeability, resulting in more space available for oxygen within the porous graphite structure and less internal resistance to oxygen flow. This situation was explored in more detail in test sets 5-8. In these test sets fiber diameter was reduced from .004 inch (test sets 1-4) to .002 inch (test sets 5-8).

Extinction by 'blowout' was observed for all thicknesses tested at both 90 knots and 70 knots (Cases 5A, 5B, 6A, 6B, 7A, 7B, 8A, and 8B). Figure 10 (Case 5A) is an example of the thermal response observed for these test cases. The reduction in fiber diameter resulted in more oxygen per unit volume and higher pore velocities than those observed for similar cases in test sets 1-4. This situation enhances convective heat transfer producing the rapid cooling depicted in Figure 10 (Case 5A). Reduction of fiber diameter had a pronounced effect

on the 0.25 inch plate and the 0.50 inch plate at both 90 knots and 70 knots. When fiber diameter was .004 inch, both plates experienced moderate combustion. When fiber diameter was reduced to .002 inch the thermal response was altered from the combustion region to the extinction by 'blowout' region.

Moderate to extensive combustion was observed in the following test cases:

- (1) Case 5C ($U_{\infty}=40$, $L=0.50$, $d=.002$, $D=.005$)
- (2) Case 5D ($U_{\infty}=10$, $L=0.50$, $d=.002$, $D=.005$)
- (3) Case 6D ($U_{\infty}=10$, $L=1.0$, $d=.002$, $D=.005$)
- (4) Case 7D ($U_{\infty}=10$, $L=0.25$, $d=.002$, $D=.005$)

Figure 11 (Case 5C) depicts an extensive combustion situation, while Figure 12 (Case 5D) presents a more moderate thermal response. In these situations it appears that the higher porosity and permeability is enhancing the combustion process by providing more oxygen. The external velocities and plate thicknesses present in these cases result in pore velocities that support combustion, but are not of sufficient magnitude so as to provide a cooling effect.

Extinction was again observed in the remaining test cases:

- (1) Case 7C ($U_{\infty}=40$, $L=0.25$, $d=.002$, $D=.005$)
- (2) Case 8C ($U_{\infty}=40$, $L=0.125$, $d=.002$, $D=.005$)
- (3) Case 8D ($U_{\infty}=10$, $L=0.125$, $d=.002$, $D=.005$)

In these cases very high pore velocities (3500 FT/HR - 55,000 FT/HR) and oxygen concentrations were present. The extinction mechanism was once again 'blowout'. It should be noted that

the second characteristic extinction mechanism, 'choking', due to insufficient oxygen to sustain combustion, was not observed for these test cases.

It was speculated that the 'choking' extinction region could be observed by conducting additional tests at greater thicknesses, thereby decreasing the pressure differential across the plate. The reduced pressure differential would produce lower average pore velocities. In order to confirm this speculation additional tests were conducted at the following thicknesses:

- (1) 2 inches
- (2) 5 inches
- (3) 8 inches

Filament diameter and ply thickness remained at .002 inch and .005 inch respectively for these tests and external velocity was 90 knots.

The 2 inch plate resulted in extensive combustion. Extinction by 'blowout' had been previously observed for all thicknesses tested at 90 knots. This result for the two inch plate confirmed the expected combustion region. Combustion initiation for the two inch plate occurred in the center region of the plate, with a cooling effect noted in the vicinity of the plate entrance. The location of the combustion initiation region indicates that the pore velocity is slightly higher than the velocity necessary to support combustion throughout the entire plate.

The five inch plate resulted in extensive combustion once again, but combustion initiation now occurred near the plate surface. This change in position of the combustion initiation region indicates that pore velocity has been reduced below the critical point where combustion would occur throughout the entire plate. These results correlate well with the results previously discussed in section IV A.

The 8 inch plate resulted in an extinction situation as a result of a 'choking' of oxygen flow. As depicted in Figure 13, oxygen concentration rapidly decreases. Slight combustion occurs near the plate entrance, but the oxygen flow is not sufficient to support even this slight combustion for an extended period of time.

The three additional thickness tests described above confirm the existence of two extinction regions and one ignition region for the more porous plate, as previously speculated.

Tests sets 5-8 indicate that decreasing filament diameter while holding other parameters constant results in an increase in both permeability and porosity. This situation typically results in either extensive combustion or extinction by 'blow-out', as described above, for plates with thicknesses of less than 1 inch. These results would indicate that permeability and porosity significantly effect the internal flow characteristics thereby controlling the thermal response of the composite plate. As previously noted, pore velocity is a function of both permeability (m) and porosity (p).

C. EFFECTS OF PERMEABILITY

In order to analyze the effects of permeability, test sets 13-16 are analyzed in comparison with test sets 1-4. The following information contrasts these two test groups:

TABLE IV: COMPARISON OF TESTS SETS 1-4 WITH TEST SETS 13-16

PARAMETERS	TEST SETS 1-4	TEST SETS 13-16
Filament Diameter	.004"	.0004"
Ply Thickness	.005"	.0005"
Permeability	$.29 \times 10^{-9} \text{ FT}^2$	$.29 \times 10^{-11} \text{ FT}^2$
Porosity	.497	.497

As can be seen from the above information, porosity remains constant while permeability decreases by a factor of 100 for test sets 13-16. It was expected that this significant reduction in permeability would alter the thermal response of the composite plate.

No combustion was observed for any of the tests conducted in test sets 13-16. Extremely low pore velocities were characteristic of all the test cases. Pore velocities ranged from .11 FT/HR for the 1.0 inch plate with an exterior velocity of 10 knots, to 134 FT/HR for a .125 inch plate with an exterior wind velocity of 90 knots. These velocities are not of sufficient magnitude to support even slight combustion. Extinction occurs in all cases as a result of 'choking' of the

oxygen flow. The 1 inch, 0.5 inch, and 0.25 inch plates, all experienced zero oxygen concentration within the plate interior. The complete depletion of oxygen occurred at the locations indicated in Table V.

TABLE V: OXYGEN DEPLETION LOCATIONS

PLATE THICKNESS	X/L-ZERO OXYGEN
1.0 inch	.03333
0.5 inch	.03333
0.25 inch	.26667

Table V indicates that for plates greater than 0.25 inch not only is pore velocity insufficient to support combustion, but permeability and pressure differential across the plate are such that oxygen does not even flow across the entire plate. This is a very desirable situation from the standpoint of combustion prevention.

A comparison of test sets 1-4 ($d=.004$ inch, $D=.005$ inch) with test sets 13-16 ($d=.0004$ inch, $D=.0005$ inch) shows the significance of permeability to the combustion process. In test sets 1-4, combustion was observed in nine of the sixteen tests conducted. In test sets 13-16, combustion was not observed in any of the tests conducted, despite the fact that porosity remained the same. These tests indicate that a minimum porosity is a necessary condition for plate combustion,

but it is not a sufficient condition. Porosity is an indicator of space available for oxygen, while permeability is a measure of the ability of a porous medium to allow flow (i.e. high permeability implies low resistance to flow). Previous tests have indicated the critical nature of pore velocity in its relationship to the combustion process. Therefore, permeability will have a significant impact on the resulting thermal response of the composite plate.

Test sets 13-16 ($d=.0004$ inch, $D=.0005$ inch) also provided some insight into the cooling process of the composite plate. Figures 14, 15, 16, and 17 depict graphite temperatures for the 1.0 inch, 0.5 inch, 0.25 inch, and 0.125 inch plates respectively. These figures indicate that plate cooling proceeds more quickly for the thinner plates. A consideration of the pore velocities and the oxygen concentrations that characterize these test cases is relevant to the cooling process. Table VI presents this information for the four plate thicknesses tested. The oxygen concentrations presented in Table VI all occurred very rapidly after the problem start time (t less than 1.0 second).

Table VI illustrates pore velocity increases as plate thickness decreases. This situation occurs because as plate thickness decreases the pressure gradient across the plate increases. The increased pressure gradient results in increased pore velocity. Despite the fact that pore velocity is increasing, it is not sufficient to support combustion, even for the 0.125

inch plate. Pore velocities of at least 500 FT/HR characterized previous test cases that experienced combustion. As can be seen from Table VI, the pore velocities for the cases under consideration are well below this value.

TABLE VI
PORE VELOCITY AND OXYGEN CONCENTRATION (TEST SETS 13-16)

PLATE SIZE	PORE VELOCITY	OXYGEN CONCENTRATION
1.0 inch	17 FT/HR	0 at X/L = .03333
0.5 inch	35.0 FT/HR	0 at X/L = .03333
0.25 inch	68.0 FT/HR	0 at X/L = .26667
0.125 inch	134.0 FT/HR	.005 lbm/FT ³ (throughout entire plate)

Even though the pore velocities experienced for these test cases were of insufficient magnitude to support combustion, it appears that they were high enough to provide some cooling to the plate through convective heat transfer. In fact, the cooling was quite significant for the 0.25 inch plate and the 0.125 inch plate as Figures 17 and 18 demonstrate.

It appears that 'choking' of oxygen flow and rapid cooling occur simultaneously for thin plates with reduced permeability. The reduced permeability provides the mechanism for preventing initial combustion by reducing pore velocity to such a level that combustion cannot be sustained. The thin plate thickness results in a pore velocity that is sufficiently high to cool

the plate through convective heat transfer. These results indicate that the composite plate designer can not only design for combustion prevention, but also for desired cooling rate. This can be accomplished by not only designing for a pore velocity such that the thermal response is in the extinction by choking region, but also designing the plate geometry such that the oxygen flow is not completely choked within the plate interior. It is believed that a threshold pore velocity exists for any particular composite plate, such that combustion will not be supported and a maximum cooling rate will be achieved.

In tests sets 9-12 ($d=.0002$, $D=.0005$) the permeability is slightly higher ($.625 \times 10^{-10} \text{ FT}^2$) than that for test sets 13-16 ($.29 \times 10^{-11} \text{ FT}^2$). This increase in permeability resulted in higher pore velocities in all test cases. This situation resulted in moving the thermal response from the extinction by 'choking' region to the combustion region for several test cases. Combustion was observed in eleven of the sixteen tests conducted for these test sets.

In all the test cases in which combustion occurred, initiation took place in the vicinity of the plate entrance. It was also observed that the combustion process was not of a robust nature, with slight to moderate combustion observed in each case. Figure 18 (case 9C) presents the thermal response of a 0.5 inch plate, with an exterior velocity of 40 knots, that is typical of the combustion process observed for these test sets. Additionally, oxygen concentration was rapidly

depleted in the vicinity of the plate entrance for all combustion situations. Figure 19 (Case 9C) depicts the oxygen depletion process observed in combustion situations. The combustion initiation region and the rapid oxygen depletion both indicate that the combustion process is immediately utilizing all oxygen available. These results indicate that the permeability is retarding the thermal response. A further increase in permeability would result in less resistance to oxygen flow, which would produce pore velocities of greater magnitude. The higher pore velocities would move the thermal response further into the combustion region, resulting in a more extensive combustion situation.

It should be noted that porosity was substantially higher in test sets 9-12 ($p=.9743$) than in test sets 1-4 ($p=.497$) and test sets 13-16 ($p=.497$). Previous tests indicated that the thermal response was not as sensitive to changes in porosity as it was to changes in permeability. In these tests though, permeability was altered with porosity. In order to completely investigate the effects of porosity, test sets 17-28 were conducted. These tests were designed to vary porosity, while holding permeability and all other input parameters constant.

D. EFFECTS OF POROSITY

Test sets 17-28 investigated the effects of varying porosity, while holding all other parameters constant. Table VII summarizes the parameters that characterize the various test sets.

TABLE VII: PARAMETERS FOR TEST SETS 17-28

TEST SETS	FILAMENT DIAMETER	PLY THICKNESS	PERMEABILITY	POROSITY
17-20	.003 inch	.004 inch	$.30 \times 10^{-9} \text{ FT}^2$.560
21-24	.006 inch	.007 inch	$.30 \times 10^{-9} \text{ FT}^2$.420
25-28	.0002 inch	.0007 inch	$.30 \times 10^{-9} \text{ FT}^2$.935

1. Test Sets 21-24 (p=.420)

As Table VII indicates, porosity and permeability for test sets 21-24 are the same order of magnitude as those experienced in test sets 1-4 ($m = .29 \times 10^{-9} \text{ FT}^2$, $p = .497$). As expected, test sets 21-24 presented thermal responses very similar to those observed for test sets 1-4. Combustion was observed in nine of the sixteen tests conducted for these sets, with combustion initiation occurring in a region removed from the plate entrance. It was also observed that the combustion process was not of a robust nature, with slight to moderate combustion observed in each ignition case. Extinction as a result of the 'choking' of oxygen flow was observed for the 1.0 inch, 0.5 inch, and 0.25 inch plates when the exterior velocity was ten knots. Extinction as a result of 'blowout' was again observed for the 0.125 inch plates at all velocities tested.

2. Test Sets 17-20 (p=.560)

In test sets 17-20, porosity was increased to .560, while permeability remained at $.30 \times 10^{-9} \text{ FT}^2$. This increase in porosity (approximately 30 percent) results in more void space available for oxygen. Combustion occurred in cases similar to those that experienced combustion in test sets 21-24. Extinction was again observed for the 1.0 inch, 0.5 inch, and 0.25 inch plates with exterior velocity equal to ten knots, and for the 0.125 inch plates at all velocities. The thermal response observed in these test sets, when combustion took place, was markedly different than that observed for the combustion cases in test sets 21-24. Extensive combustion was observed in several instances, especially for the 0.25 inch and the 0.50 inch plates. Figures 20 (Case 17A) and 21 (Case 19A) are typical of the thermal response observed.

It appears that the increase in porosity from .420 (test sets 21-24) to .560 (test sets 17-20) did not induce combustion to occur in any additional test cases, but it did impact on the thermal response. The combustion process is of a more robust nature. The additional space available for oxygen supports the combustion process once it initiates.

3. Test Sets 25-28 (p=.935)

In tests sets 25-28, porosity is increased to .935, indicating a great deal of void space available for oxygen. Combustion was again observed in several instances. The significant increase in porosity produced a dramatic change in

the speed of the observed thermal response. Figure 22 (Case 25B) is indicative of the rapid thermal response observed when combustion took place in these high porosity tests, as Figure 22 depicts, graphite temperatures in excess of 1250°F are achieved in less than 0.25 seconds. These tests again indicate that an increase in porosity does not induce combustion to occur in any additional test situations, but it does impact on the nature of the thermal response. High porosity (p greater than 0.90) appears to result in rapid, extensive combustion situations if permeability is such that pore velocity will support the combustion process and allow combustion to initiate.

In summary, it is thought that permeability, and its associated impact on pore velocity, determines whether the thermal response will be located in the combustion region or in one of the two extinction regions that exist on either side of the combustion region (extinction by 'choking' of oxygen flow or extinction by 'blowout'). If the thermal response is located in the combustion region, it is thought that porosity controls the speed and robustness of the combustion process.

E. EFFECTS OF EXTERIOR VELOCITY

Exterior velocity is the driving force for the internal oxygen flow that is required for both the combustion and the extinction processes. Even though exterior velocity provides

this driving force, neither extremely high nor extremely low velocities are sufficient to guarantee extinction. Previous discussion has indicated that pore velocity is a critical factor in analyzing the thermal response. Permeability, plate thickness, and porosity are all factors which can control and alter interior pore velocity to such an extent that the thermal response may be contrary to preconceived expectations based solely on the knowledge of exterior velocity.

Exterior velocity does appear to effect the combustion initiation region. In several test cases, with high exterior velocities (i.e. 90 knots) initial combustion was observed in the latter half of the plate, while in those cases with low exterior velocities, initial combustion occurred in the proximity of the plate surface. These results indicate that even though plate geometry results in a pore velocity that supports combustion, the exterior velocity is controlling where the initial combustion will occur. High exterior velocities result in oxygen flow that provides cooling at the plate entrance. Initial combustion then occurs in the latter plate regions after the oxygen temperature has reached a sufficient level so that heat generation overcomes convective heat transfer. Figure 5 depicts combustion initiation in the latter plate regions.

Low exterior velocities are not sufficient to produce the initial cooling effects described above. If the pore velocities are sufficient to support combustion, ignition will commence in the proximity of the plate surface.

In those situations in which extinction occurs as a result of 'blowout', higher cooling rates were observed with higher exterior velocities. This result was as expected.

V. CONCLUDING REMARKS

The test results indicate that permeability, porosity, filament diameter, plate thickness, and exterior wind velocity all have significant effects on the combustion process. In attempting to understand the thermal response of a composite plate, it must be realized that two extinction regions exist on either side of a combustion region. Figure 23, depicts this situation. For a given temperature, say $T = 1050^{\circ}\text{F}$, extinction will result for pore velocities less than u_{pA} or for pore velocities greater than u_{pC} . For $u_{pA} < u_p < u_{pC}$, combustion will result for all $T > 1050^{\circ}\text{F}$. Thus for a given temperature, and fixed design, there is extinction at low pore velocities ($u_p < u_{pA}$), followed by combustion for $u_{pA} < u_p < u_{pC}$, and again followed by extinction for $u_p > u_{pC}$.

For pore velocities less than u_{pA} , the system is air poor, and extinction occurs because heat generation is less than the heat transferred out of the system as a result of convection. As u_p is increased beyond u_{pA} , heat generation exceeds heat transferred and combustion with increasing system temperature will occur. The minimum ignition temperature occurs at $u_p = u_{pB}$. Increasing u_p above u_{pB} results in increasing ignition temperatures. For pore velocities greater than u_{pC} , extinction will occur once again since heat transferred exceeds heat generated.

At this point, the system is air rich. That is, there is an excess of oxygen above what is required to sustain combustion and 'blowout' will occur.

It has been established that an ignition curve similar to that discussed above for Figure 23 exists for any composite plate. Average pore velocity is selected as the abscissa for the curve because of the profound effects observed as a result of variation of this parameter during the test runs. Average pore velocity is influenced by exterior wind velocity, plate thickness, and interior plate geometry.

If a composite plate is designed to retard combustion by 'choking' of oxygen flow, then high exterior velocities are not desirable because they may be of such magnitude that the thermal response is moved from the 'choking' extinction region to the combustion region. Similarly, if the designer intends combustion prevention to be achieved as a result of 'blowout', high exterior velocities would be desirable. In short, the goals of the composite material designer must be understood if combustion is to be prevented and a desirable cooling rate of the porous graphite structure is to be achieved.

Additional, extensive testing is required in order to further quantify the thermal response of composite plates of various geometries. Tests conducted with additional exterior wind velocities and under different initial conditions are also required. An exploration of the ignition process may prove enlightening. This task could be accomplished by beginning

with an extinction situation and gradually increasing initial graphite temperature for each successive computer test run. Combustion initiation could be observed along with the robustness of the combustion process.

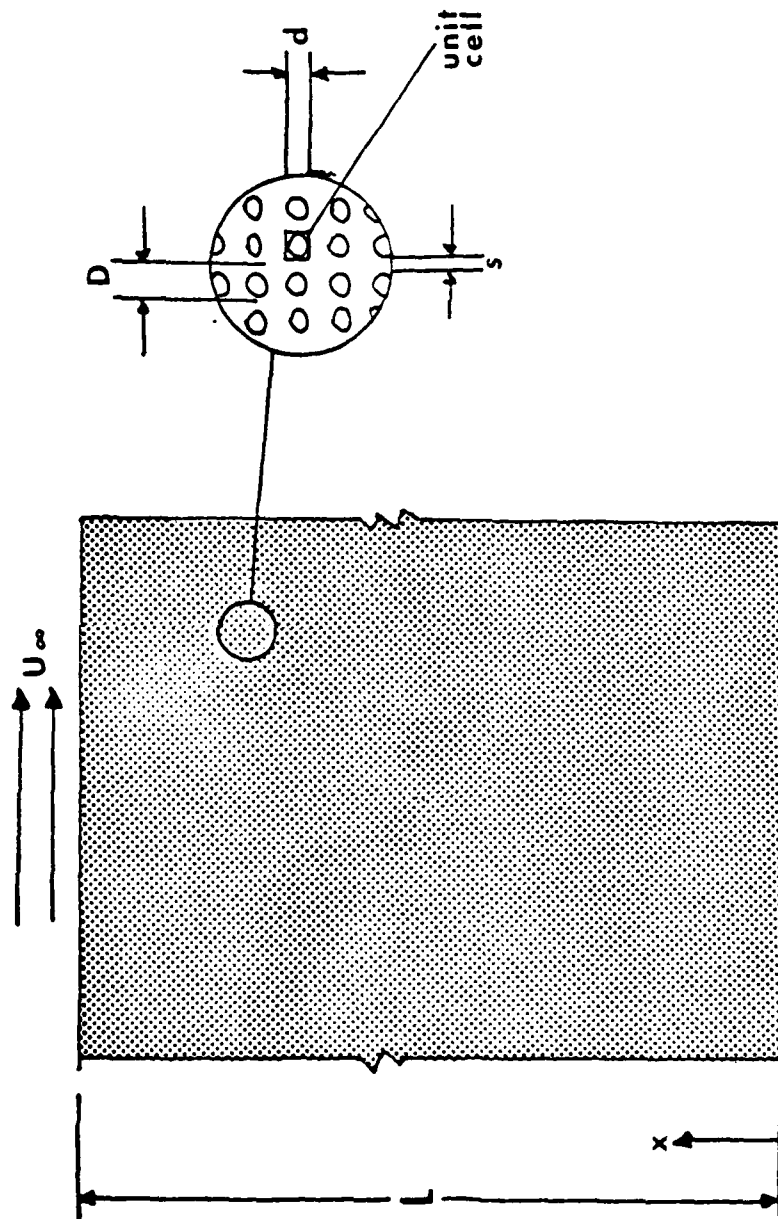


FIGURE 1. Idealized Geometry of a Fibrous Graphite Plate.

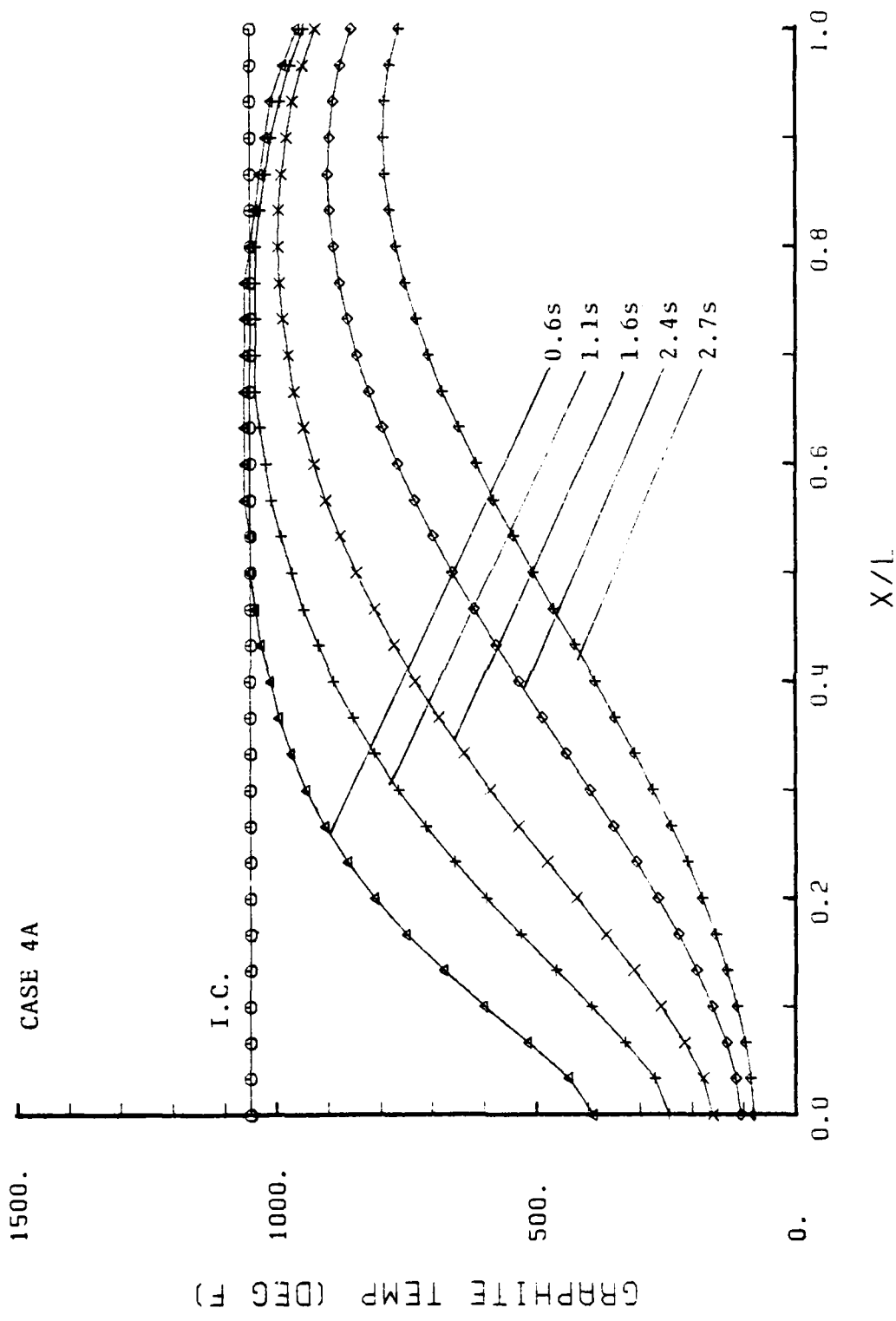


FIGURE 2. Graphite Temperature - Case 4A ($U_{\infty}=90KT$; $d=.004''$; $D=.005''$; $L=.125''$).

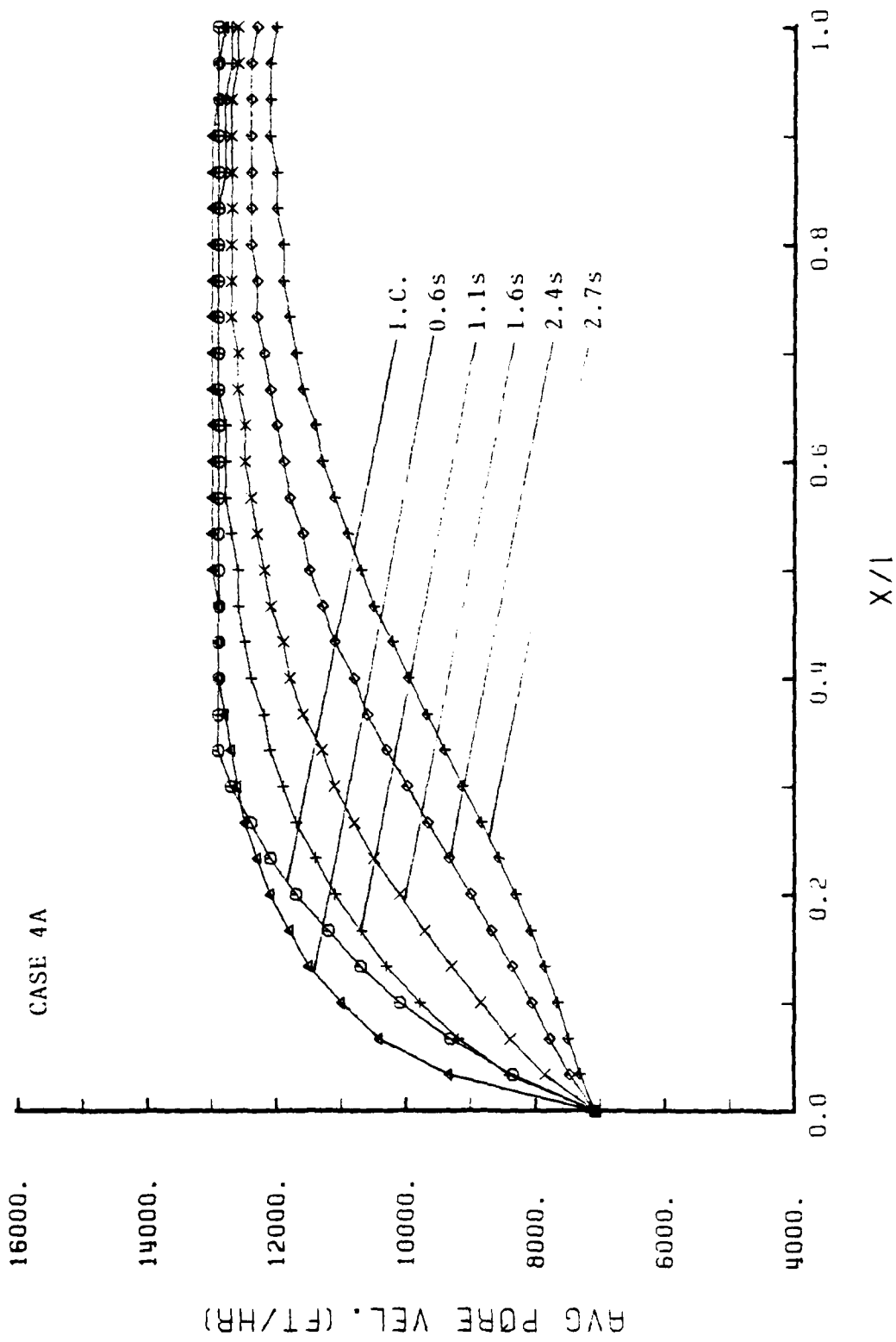


FIGURE 3. Average Pore Velocity - Case 4A ($U_{\omega} = 90KT$; $d = .004$ "; $d = .005$ "; $L = .125$ ").

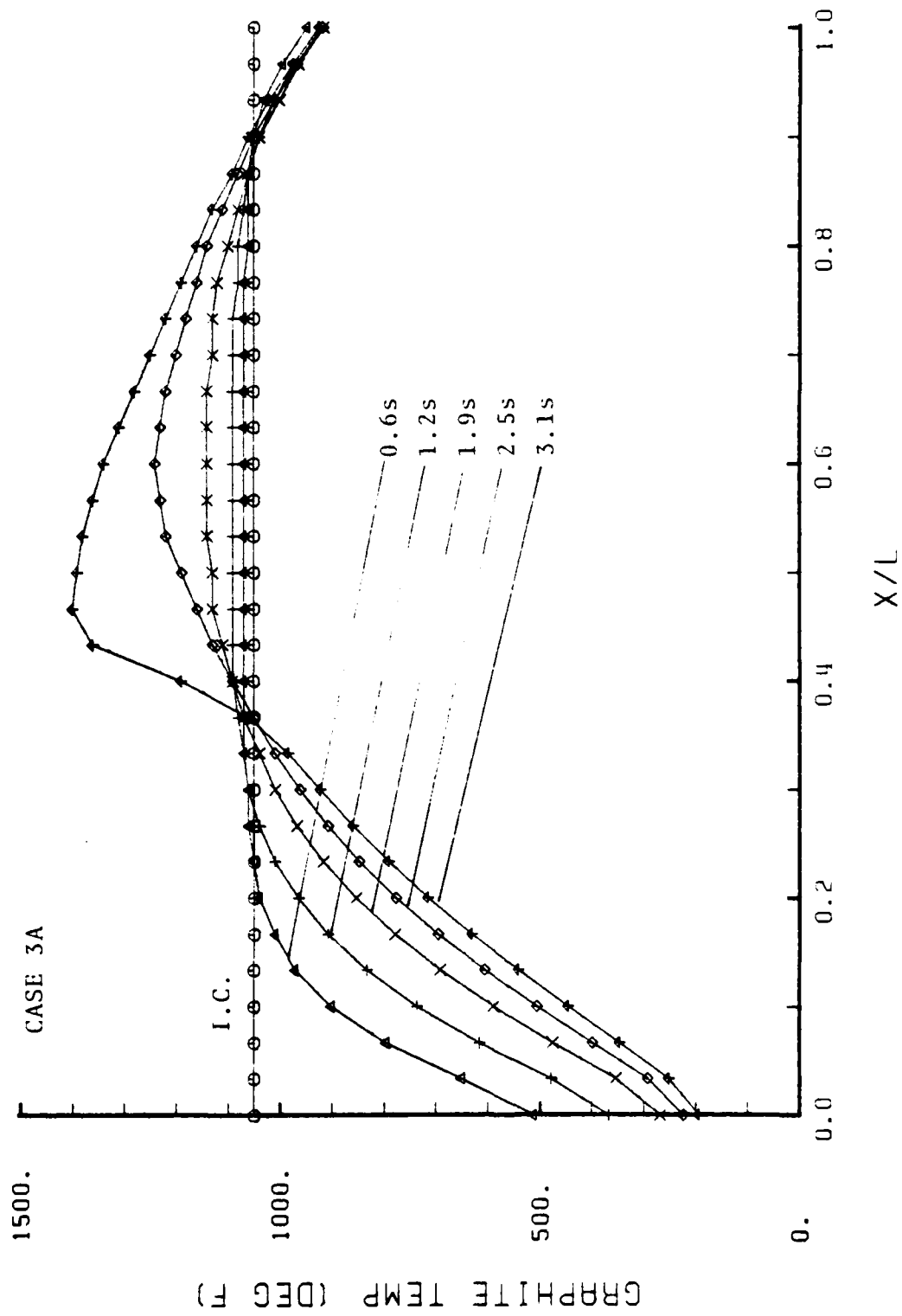


FIGURE 4. Graphite Temperature - Case 3A ($U_{\infty} = 90\text{KT}$; $d = .004''$; $D = .005''$; $L = .25''$).

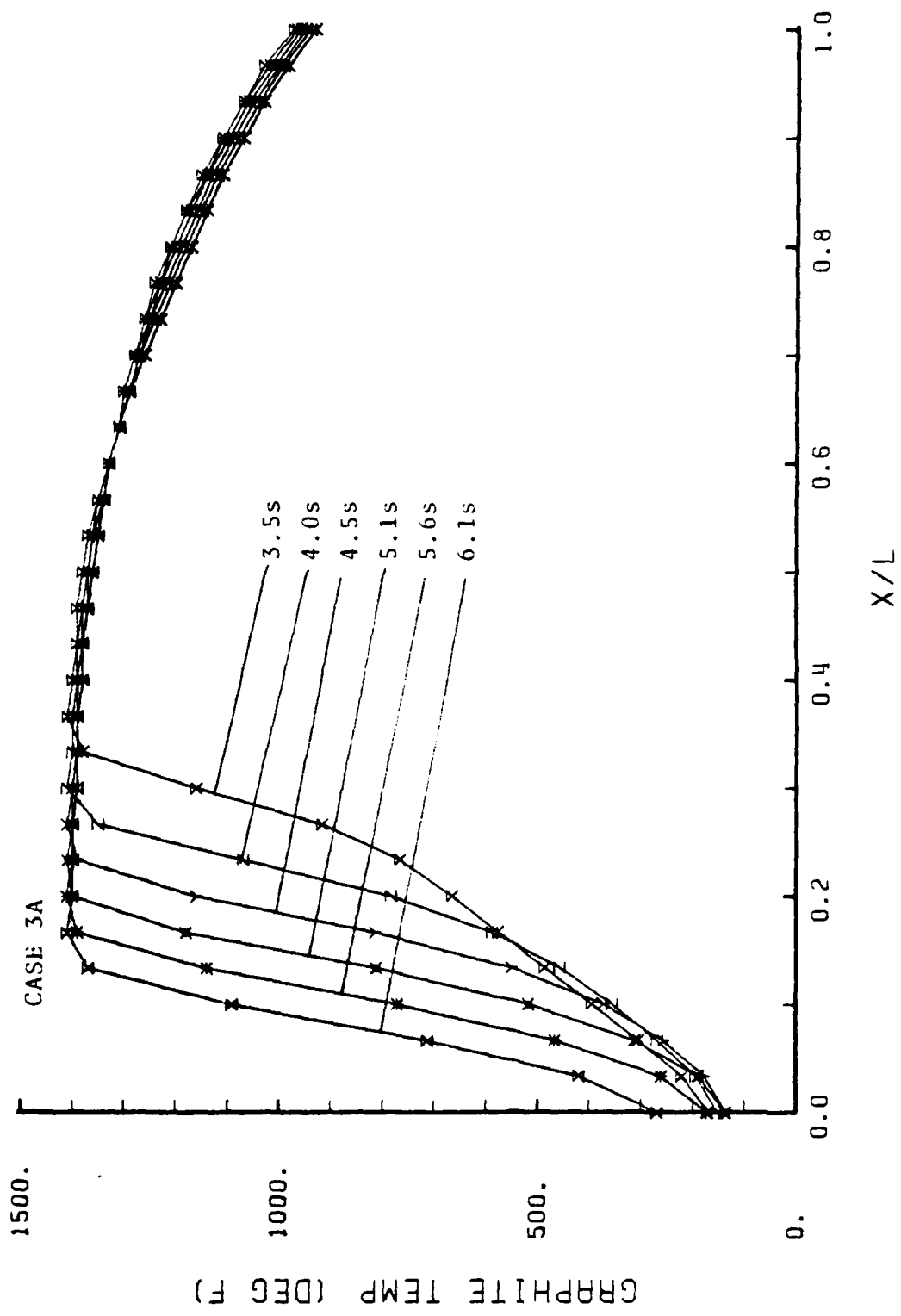


FIGURE 5. Graphite Temperature - Case 3A ($U_{\infty}=90\text{KT}$; $d=.004''$; $D=.005''$; $L=.25''$).

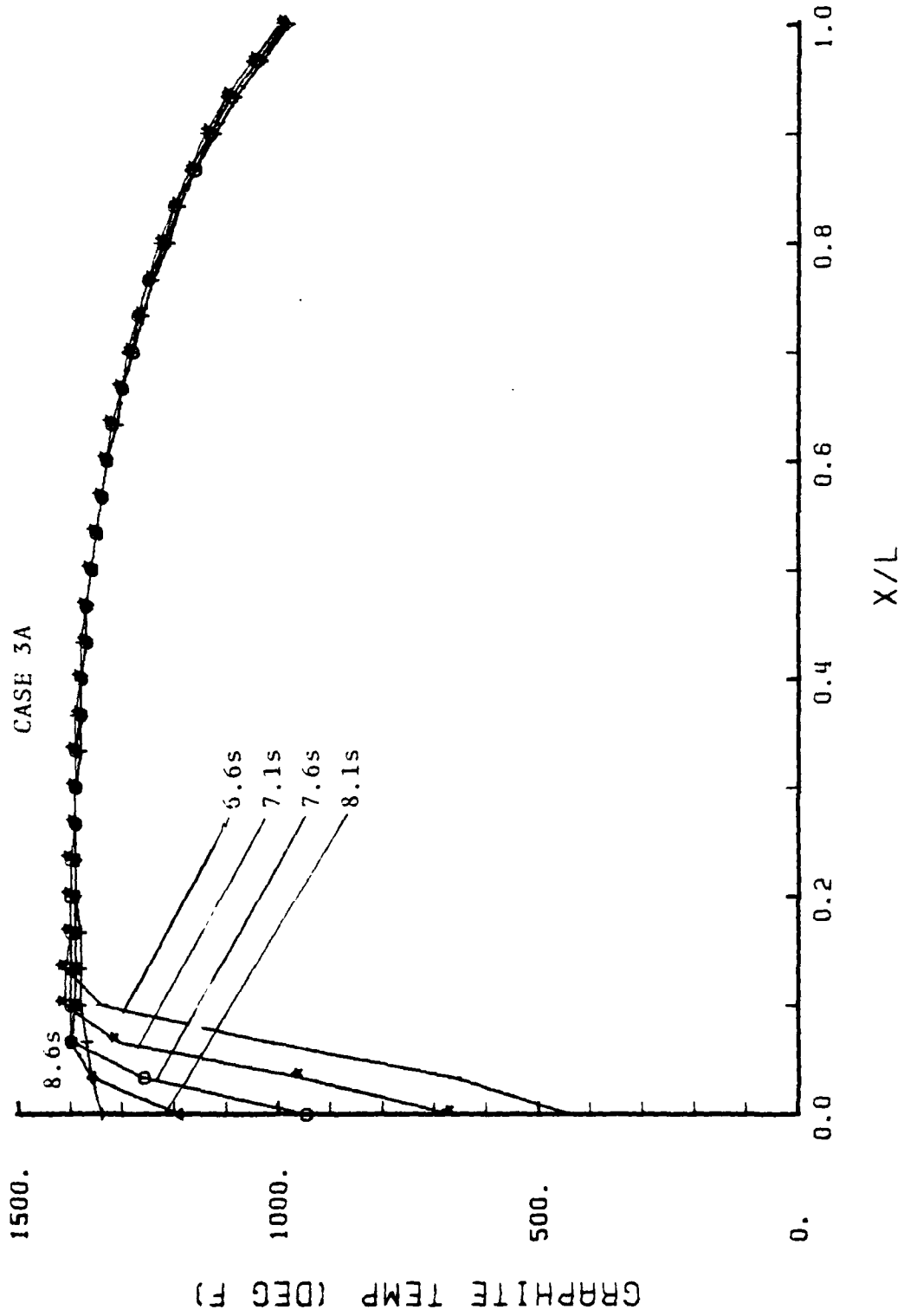


FIGURE 6. Graphite Temperature - Case 3A ($U_{\infty} = 90\text{KT}$; $d = .004''$; $D = .005''$; $l = .25''$).

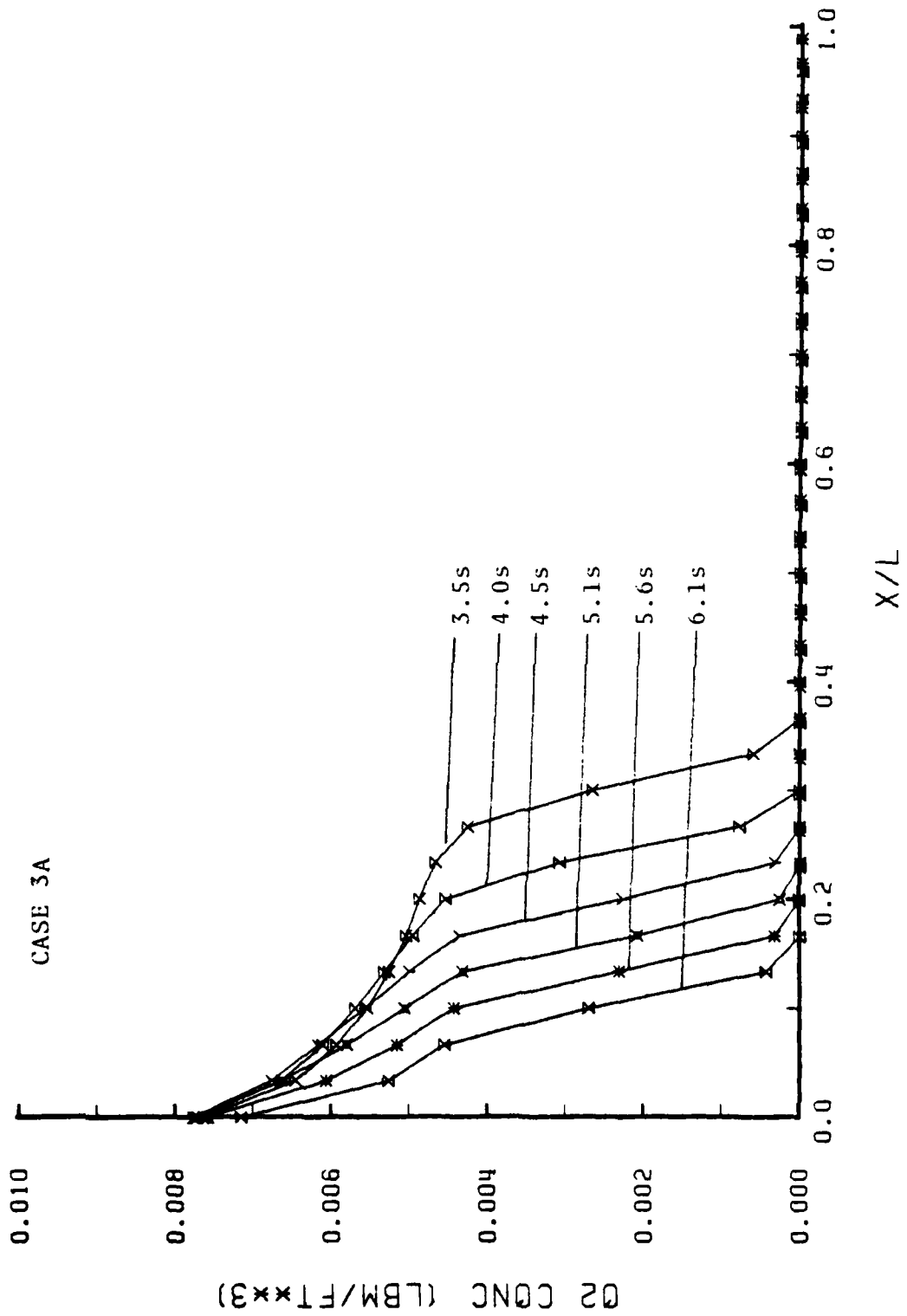


FIGURE 7. Oxygen Concentration - Case 3A ($U_{\infty}=90$ KTS; $d=.004$ " ; $D=.005$ " ; $L=.25$ ").

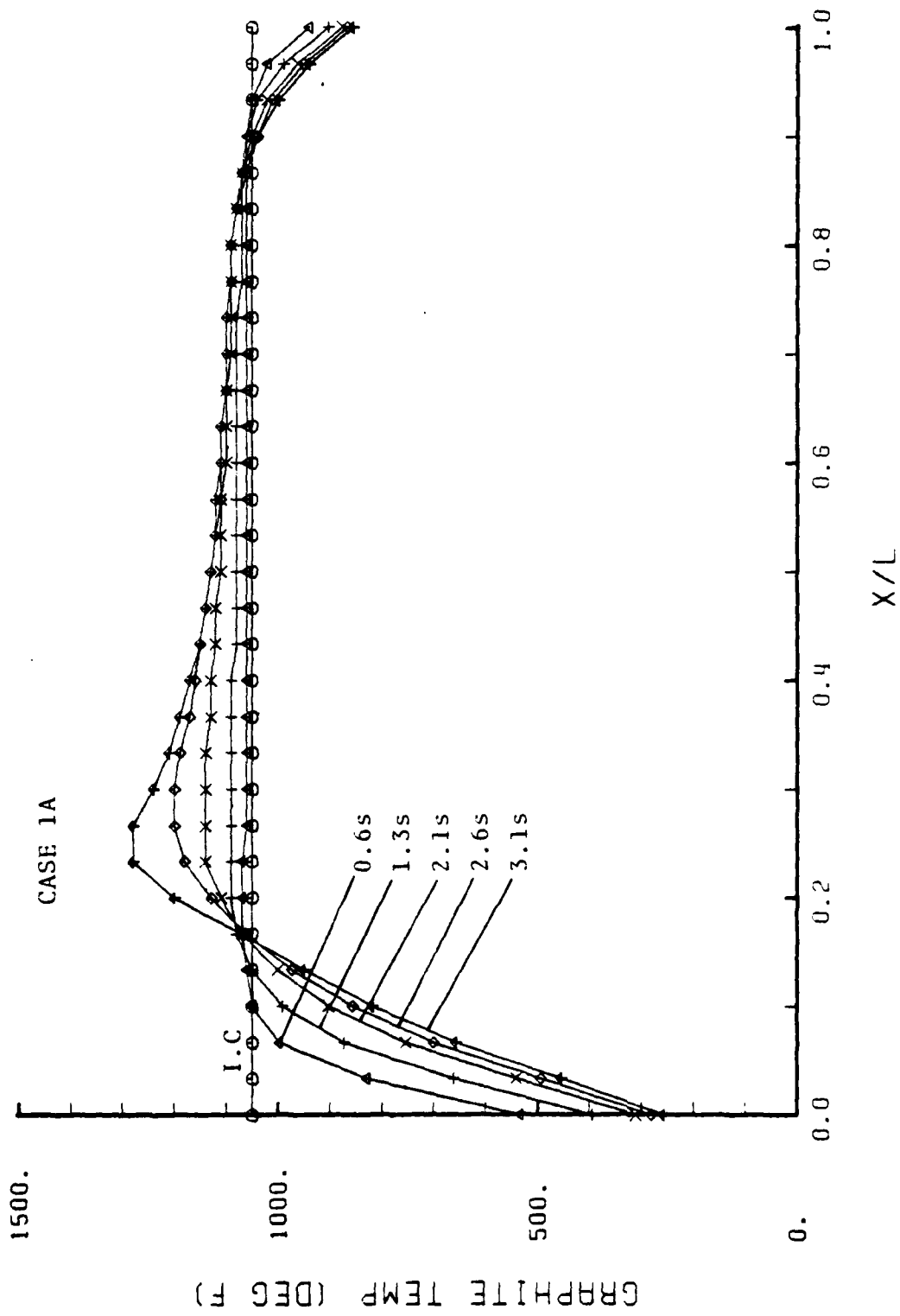


FIGURE 8. Graphite Temperature - Case 1A ($U_{\infty}=90KT$; $d=.004''$; $D=.005''$; $L=0.5''$).

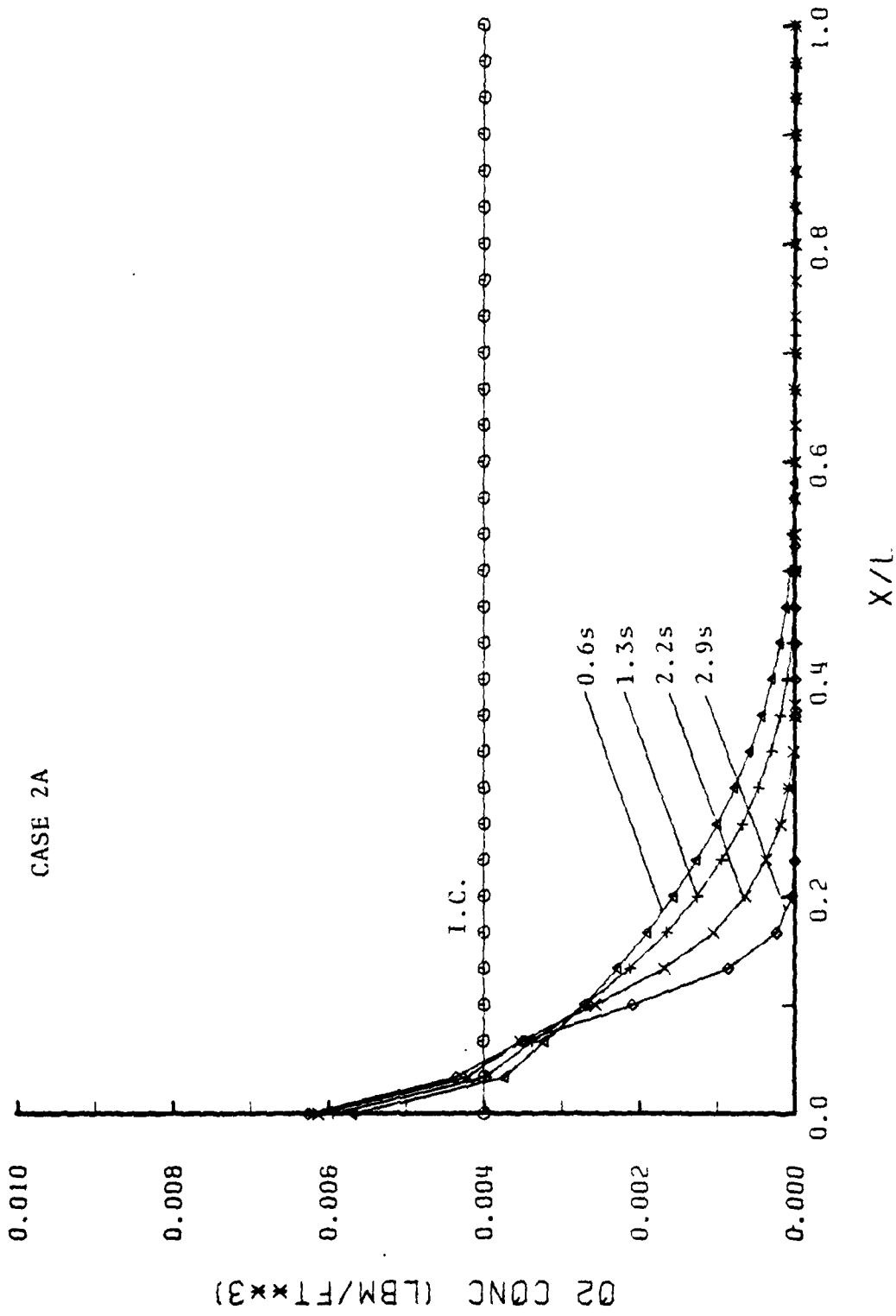


FIGURE 9. Oxygen Concentration - Case 2A ($U_{\infty}=90\text{KTS}$; $d=.004''$; $D=.005''$; $L=1.0''$).

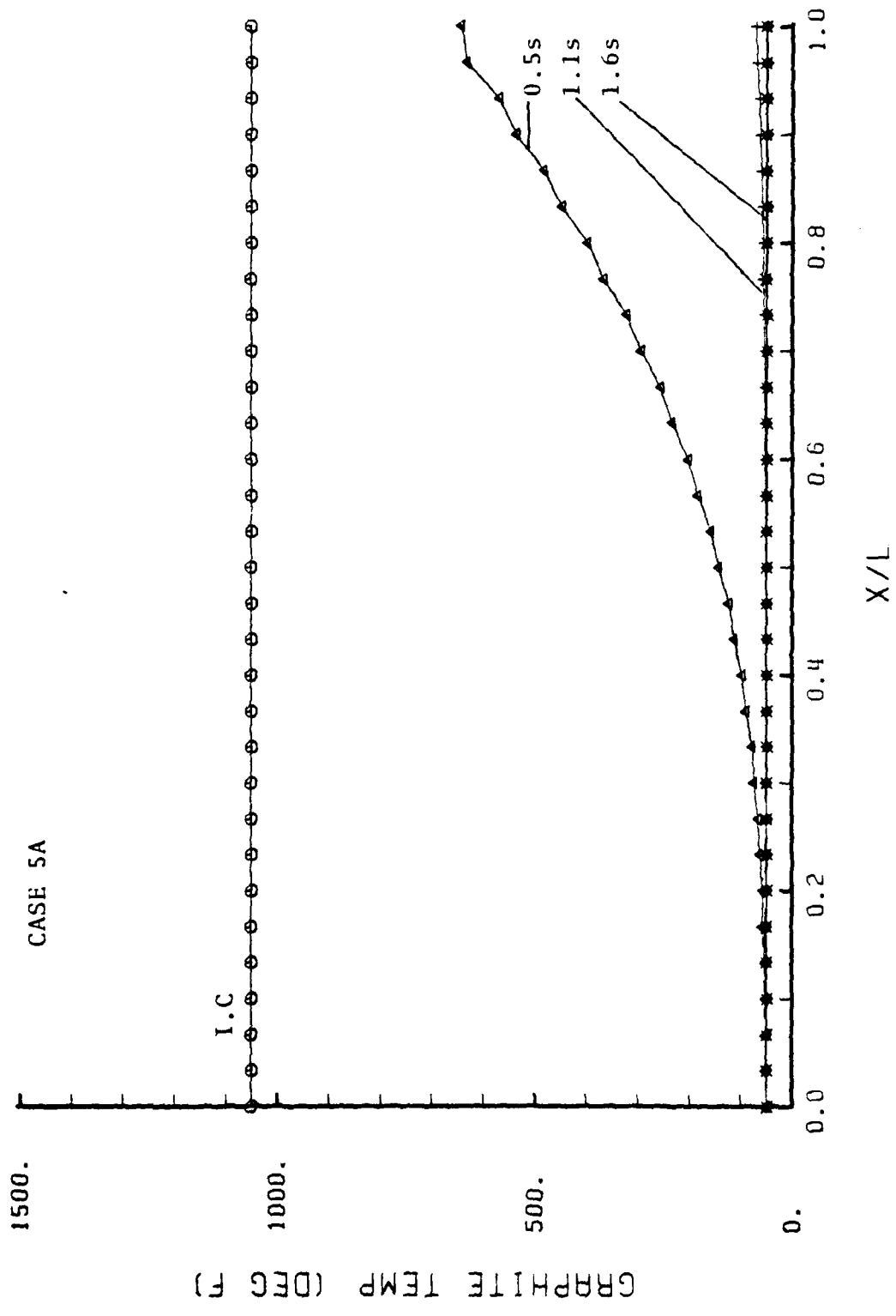


FIGURE 10. Graphite Temperature - Case 5A ($U_{\infty}=90KT$; $d=.001^{\circ}$; $D=.005^{\circ}$; $L=0.5^{\circ}$).

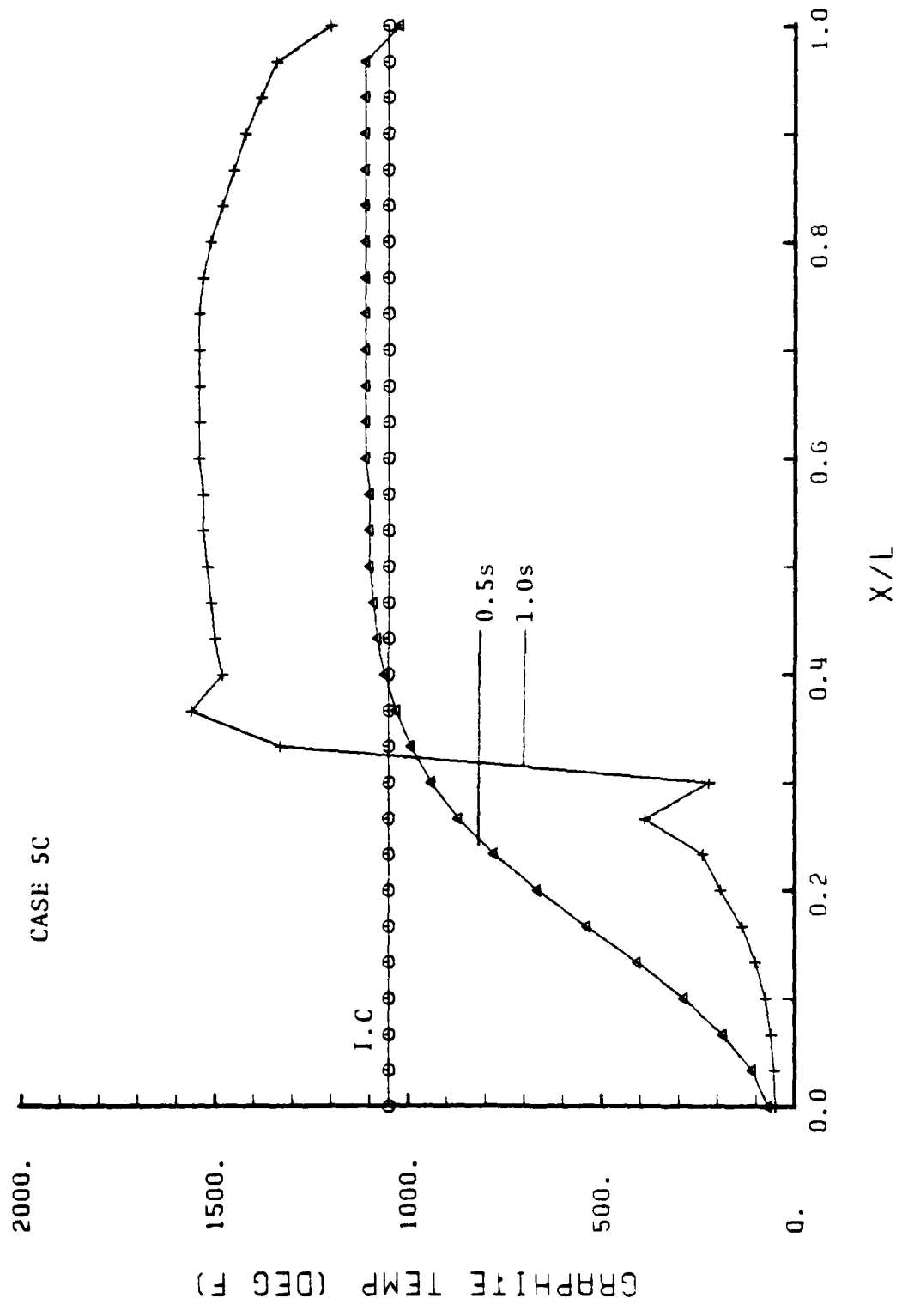


FIGURE 11. Graphite Temperature - Case 5C (U_{∞} 40KT; $d=.002''$; $D=.005''$; $L=0.5''$).

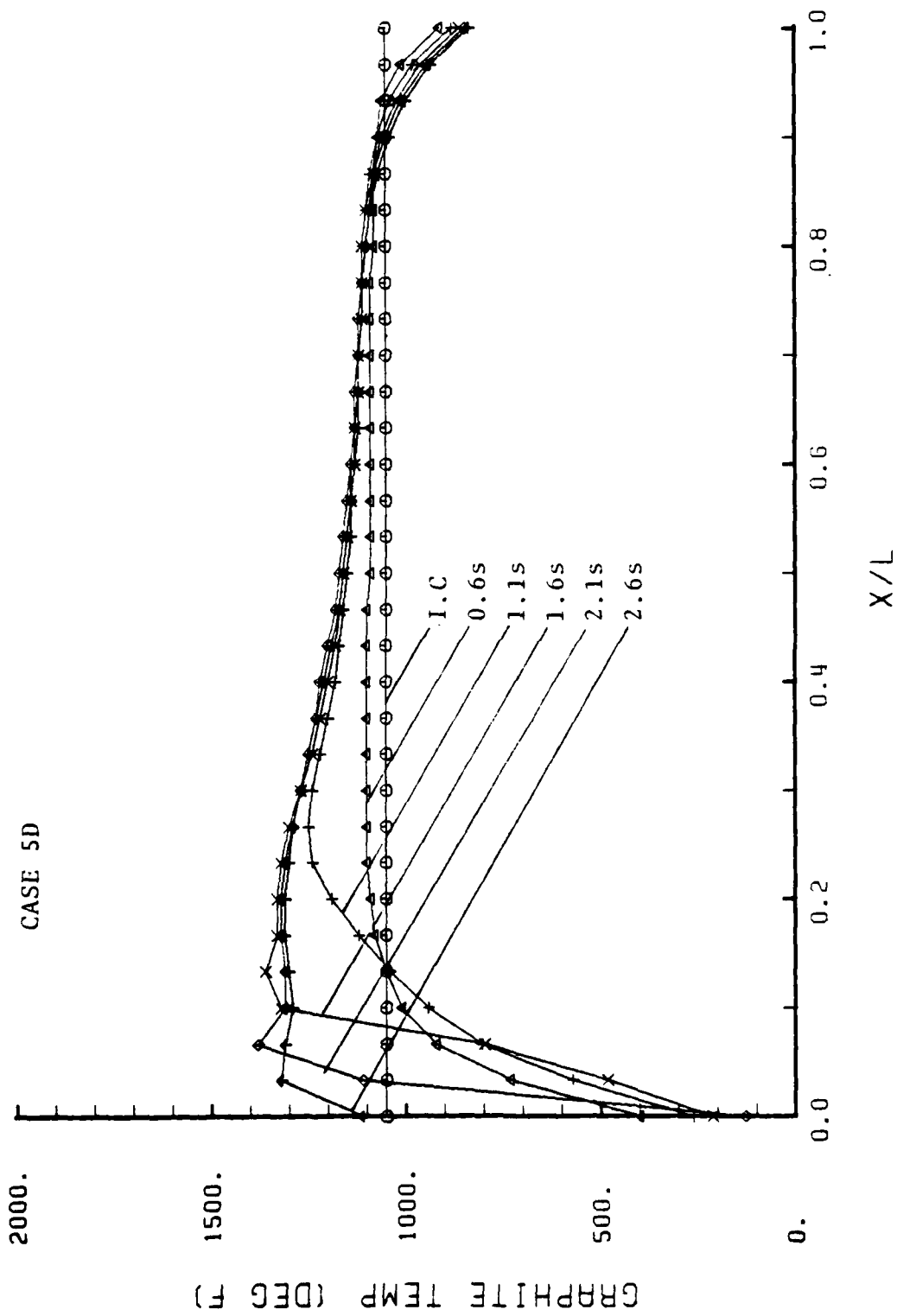


FIGURE 12. Graphite Temperature - Case 5D ($U_{\infty} = 10KT$; $d = .002''$; $D = .005''$; $L = 0.5''$).

8 INCH PLATE THICKNESS TEST

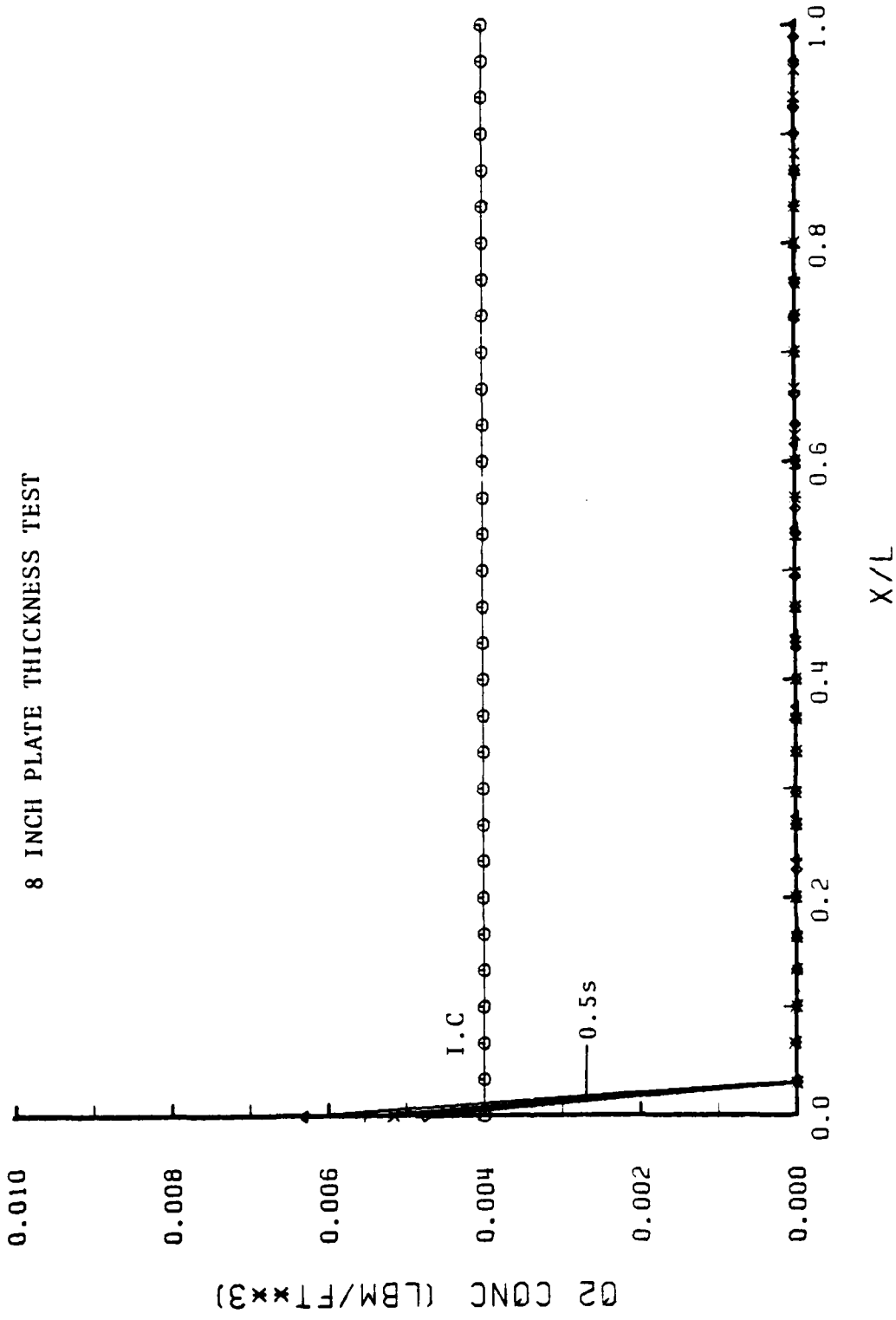


FIGURE 13. Oxygen Concentration ($U_{\infty} = 90KT$; $d = .002''$; $D = .005''$; $L = 8.0''$).

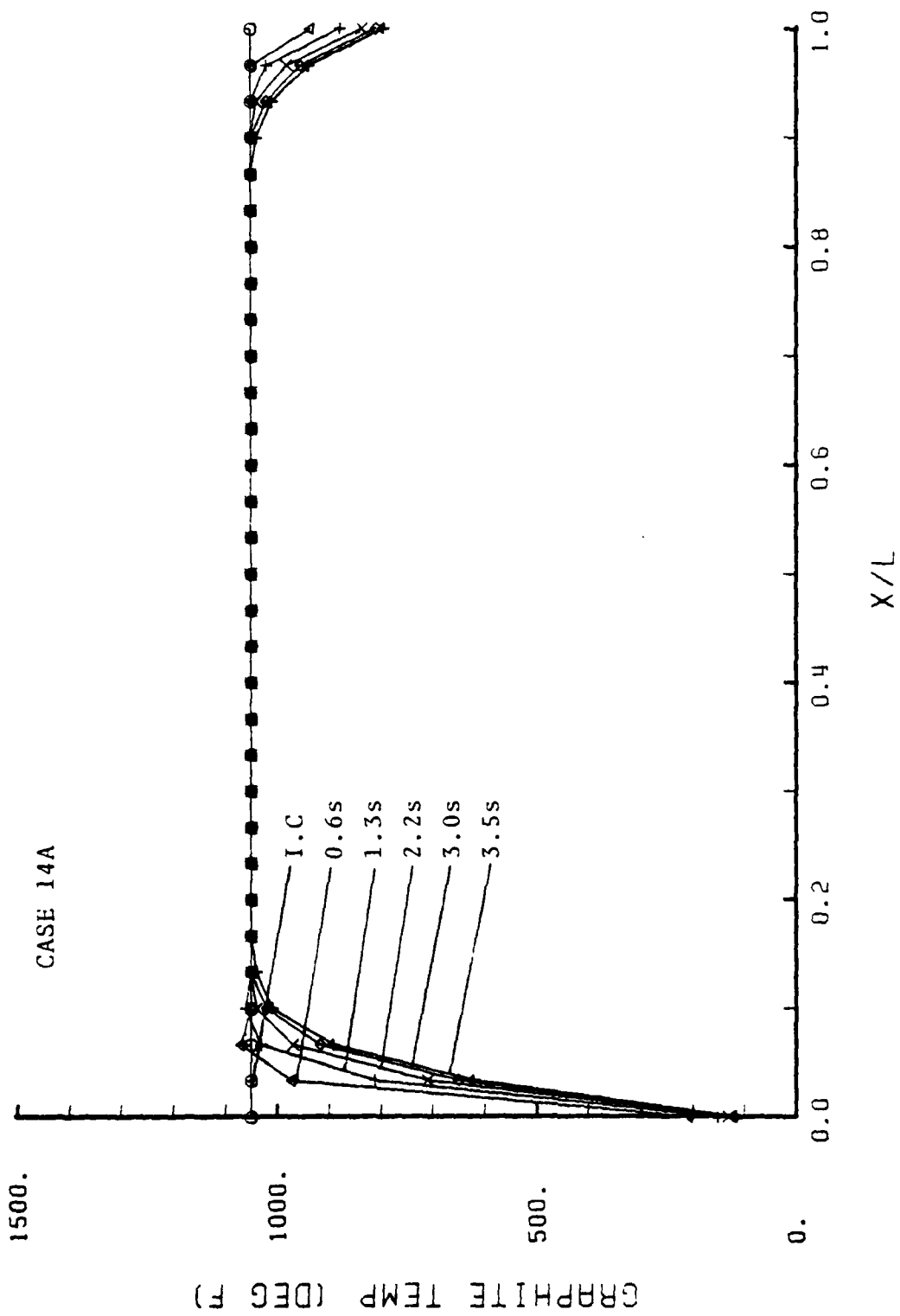


FIGURE 14. Graphite Temperature - Case 14A ($U_{\infty}=90KT$; $d=.0004''$; $D=.0005''$; $L=1.0''$).

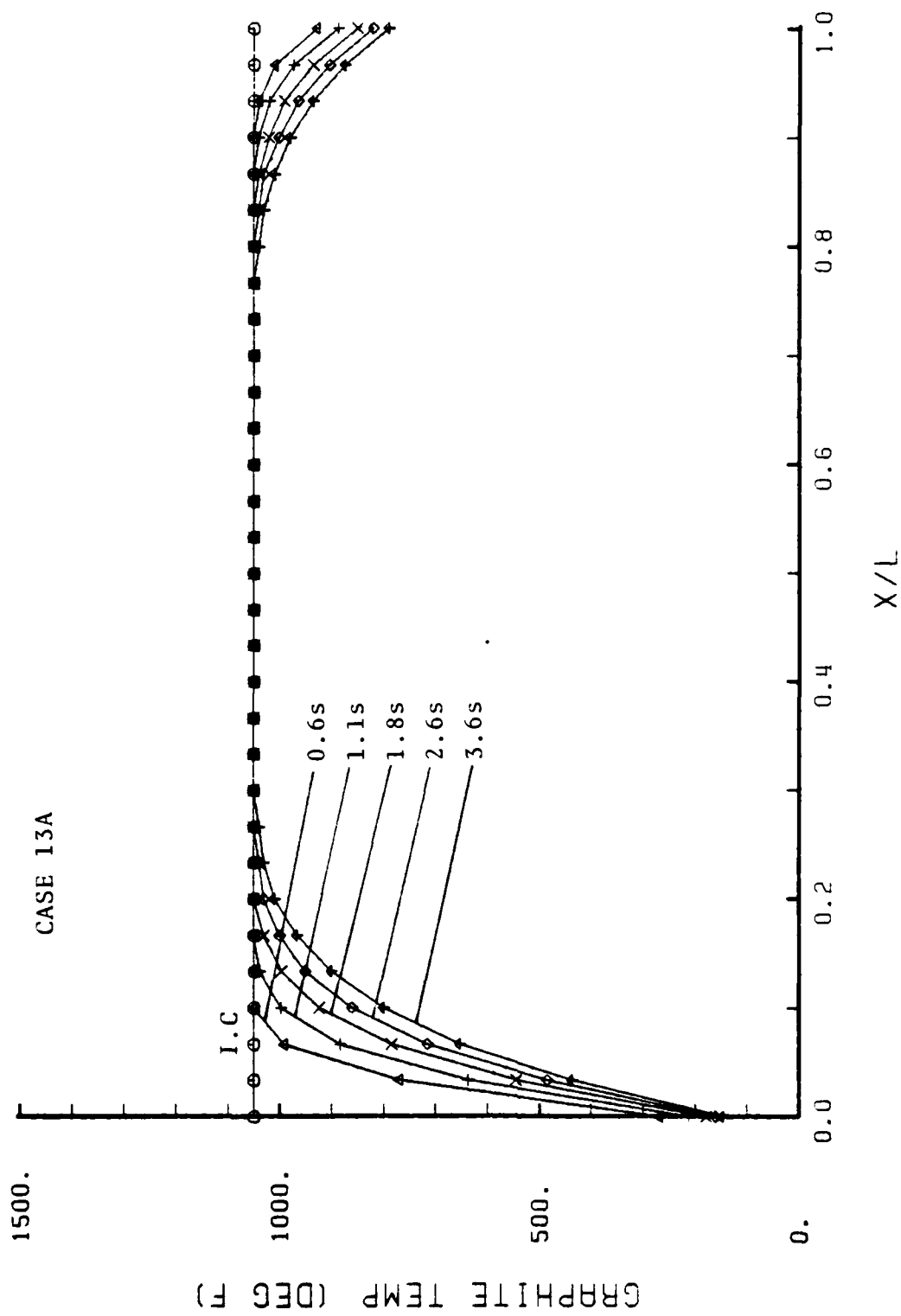


FIGURE 15. Graphite Temperature - Case 13A ($U_{\infty} = 90\text{KT}$; $d = .0004''$; $D = .0005''$; $L = 0.5''$).

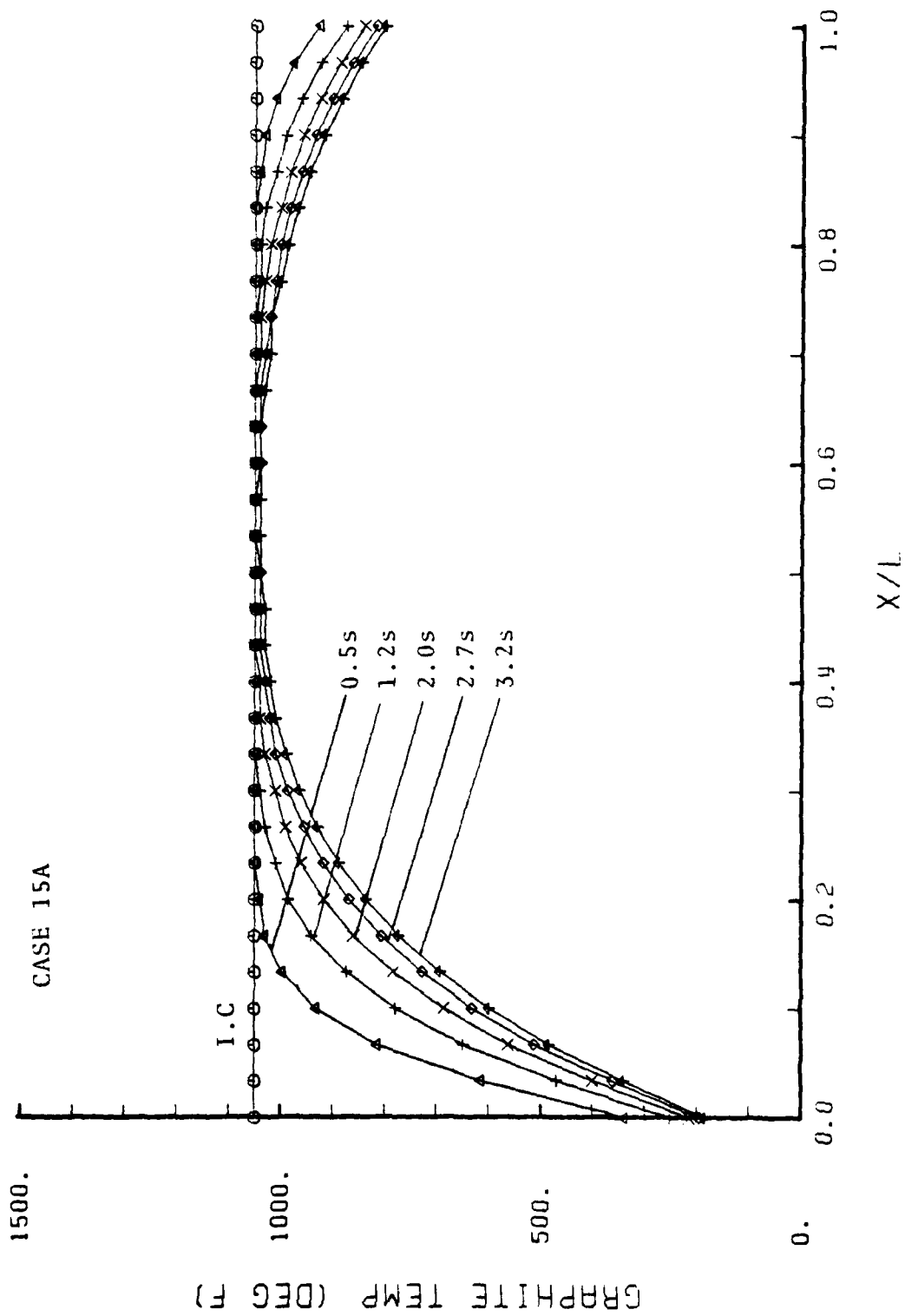


FIGURE 16. Graphite Temperature - Case 15A ($U_{\infty}=90\text{KTS}$; $d=.0004''$; $D=.0005''$; $L=0.25''$).

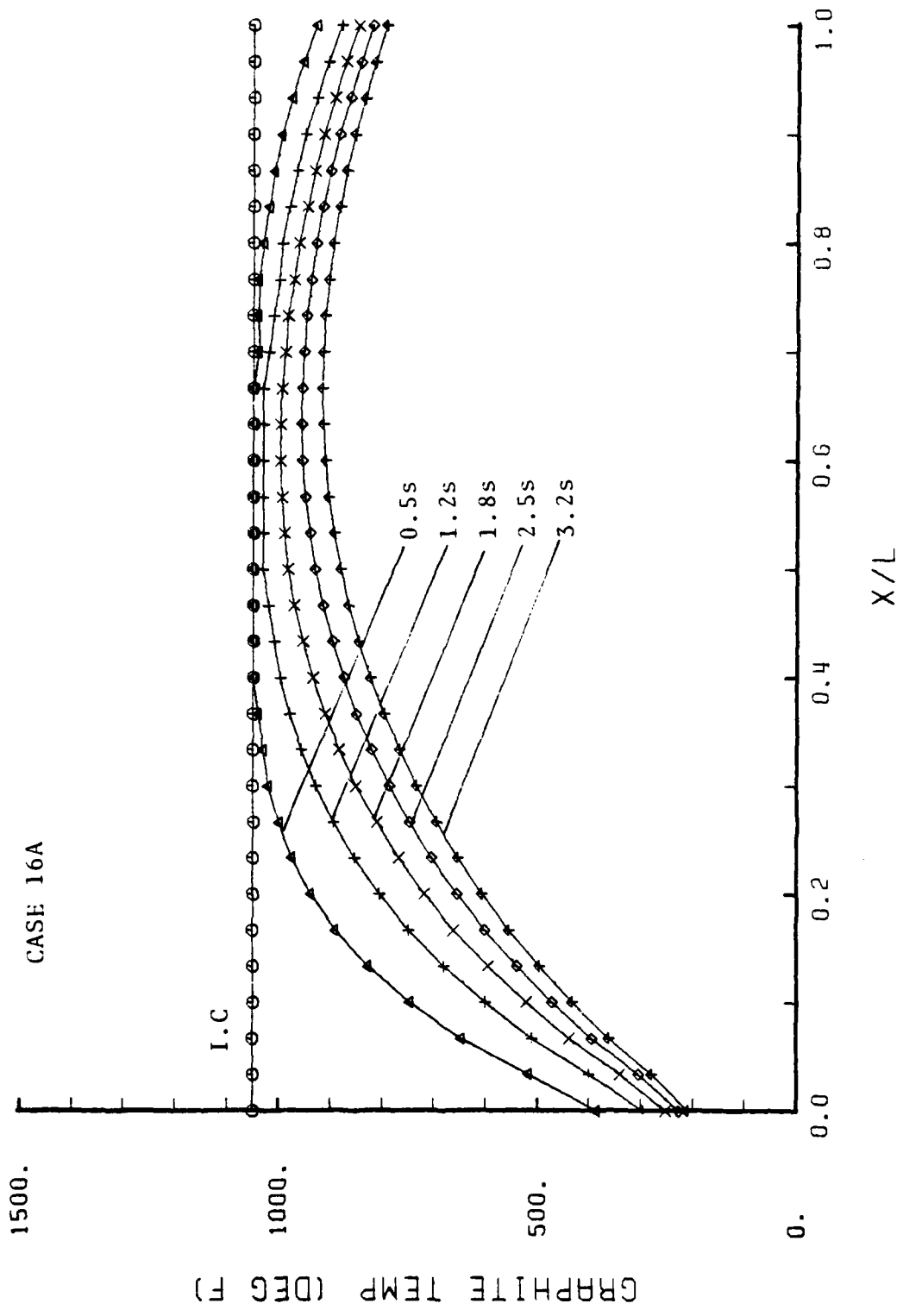


FIGURE 17. Graphite Temperature - Case 16A ($U_{\infty} 90KT$; $D=.0004''$; $D=.0005$; $L=0.125''$).

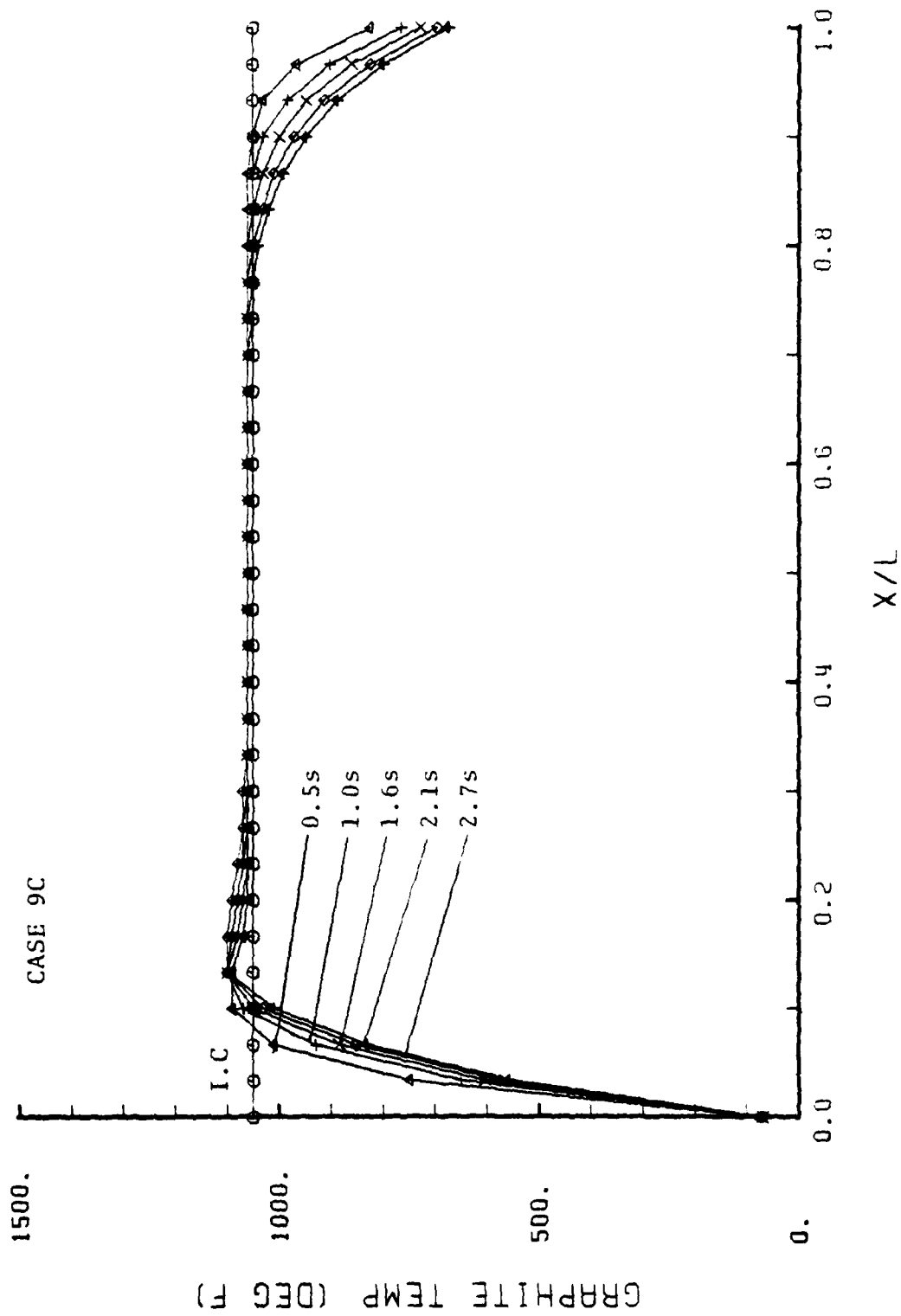


FIGURE 18. Graphite Temperature - Case 9C ($U_{\infty} = 40 \text{KT}$; $d = .0002''$; $D = .0005''$; $L = 0.5''$).

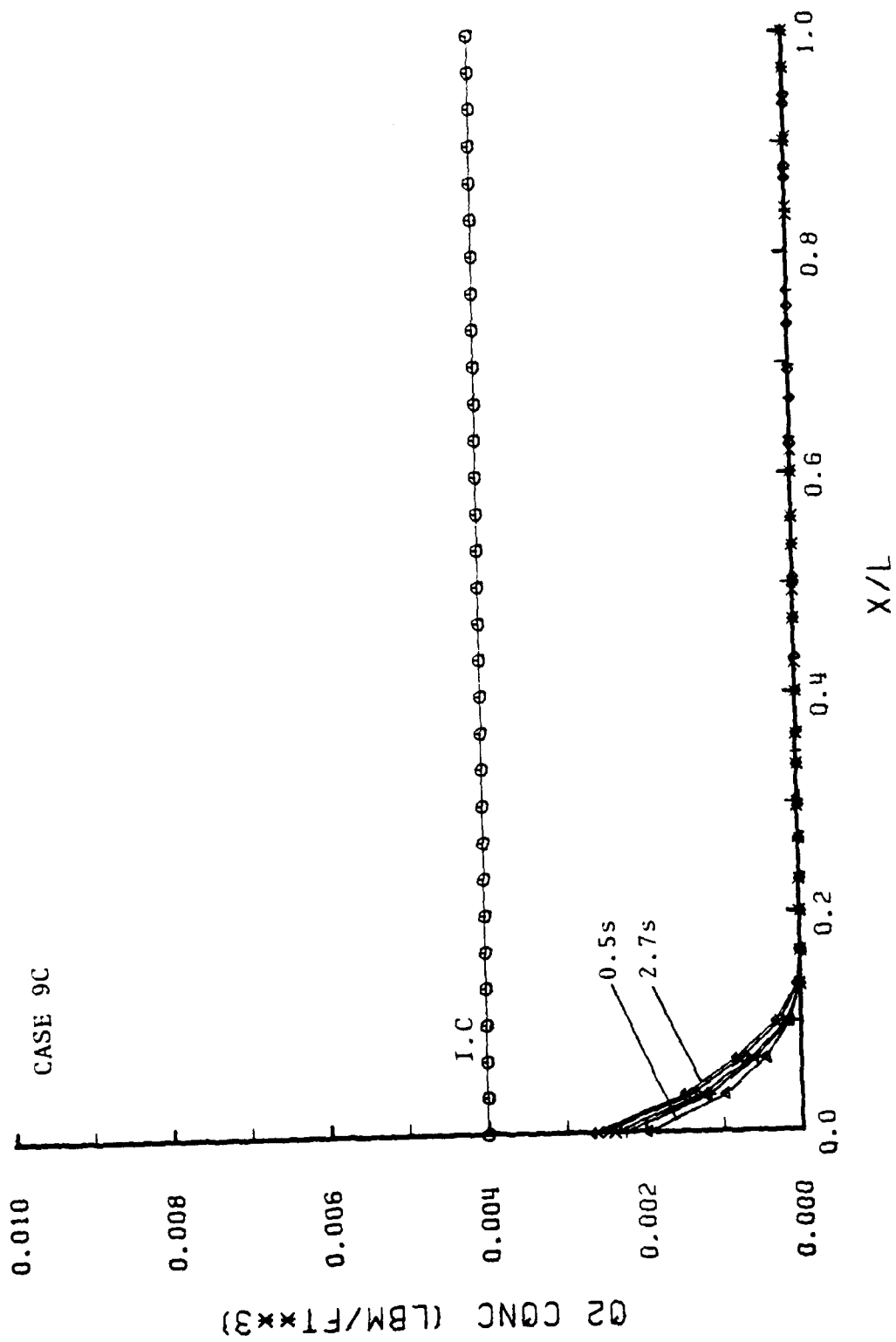


FIGURE 19. Oxygen Concentration - Case 9C ($U_{\infty} = 40KT$; $d = .0002$ "; $D = .0005$ "; $L = 0.5$ ").

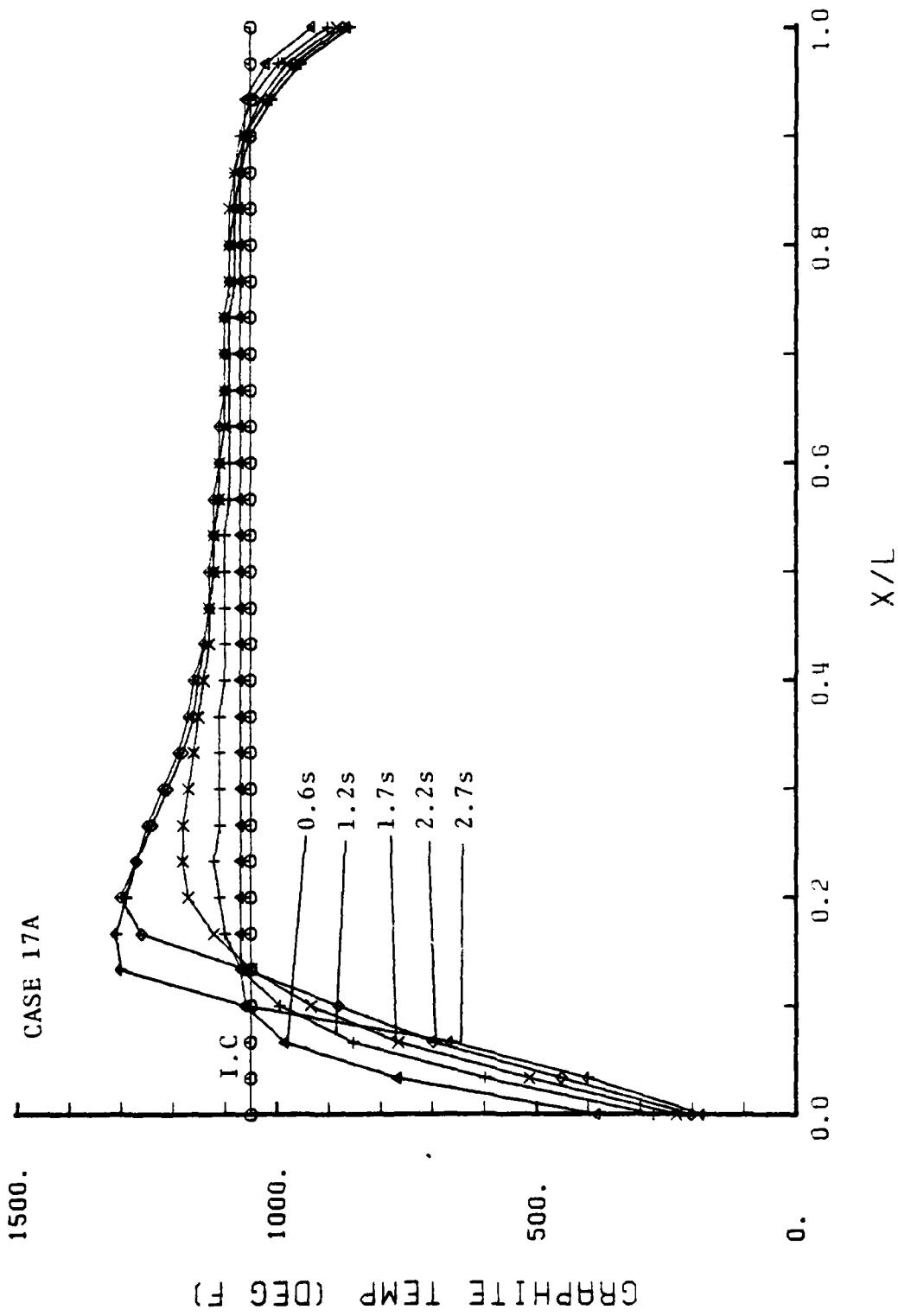


FIGURE 20. Graphite Temperature - Case 17A ($U_{\infty} = 90\text{KT}$; $d = .003''$; $D = .004''$; $L = 0.5''$).

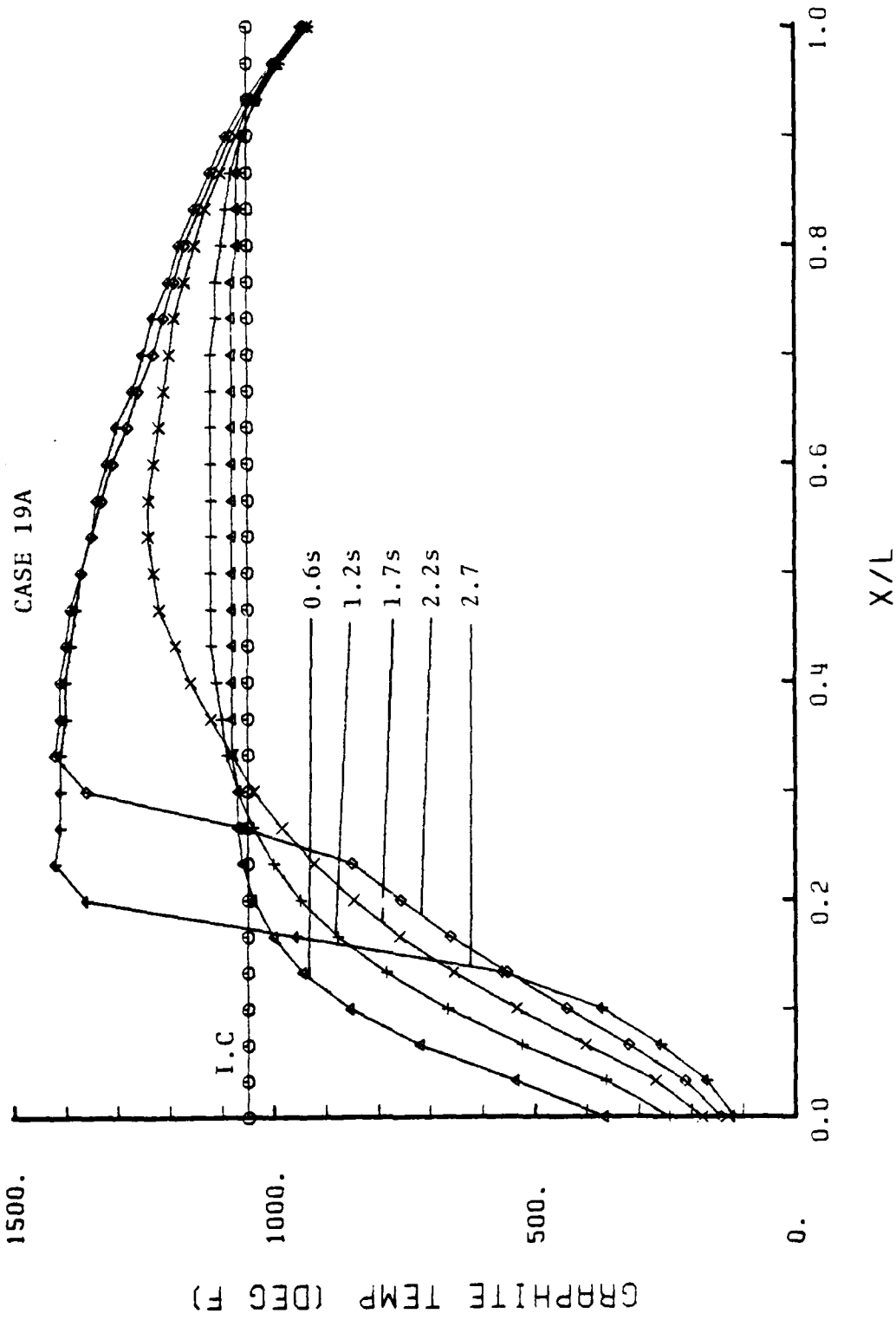


FIGURE 21. Graphite Temperature - Case 19A ($U_{\infty}=90\text{KT}$; $d=.003''$; $D=.004''$; $L=0.25''$).

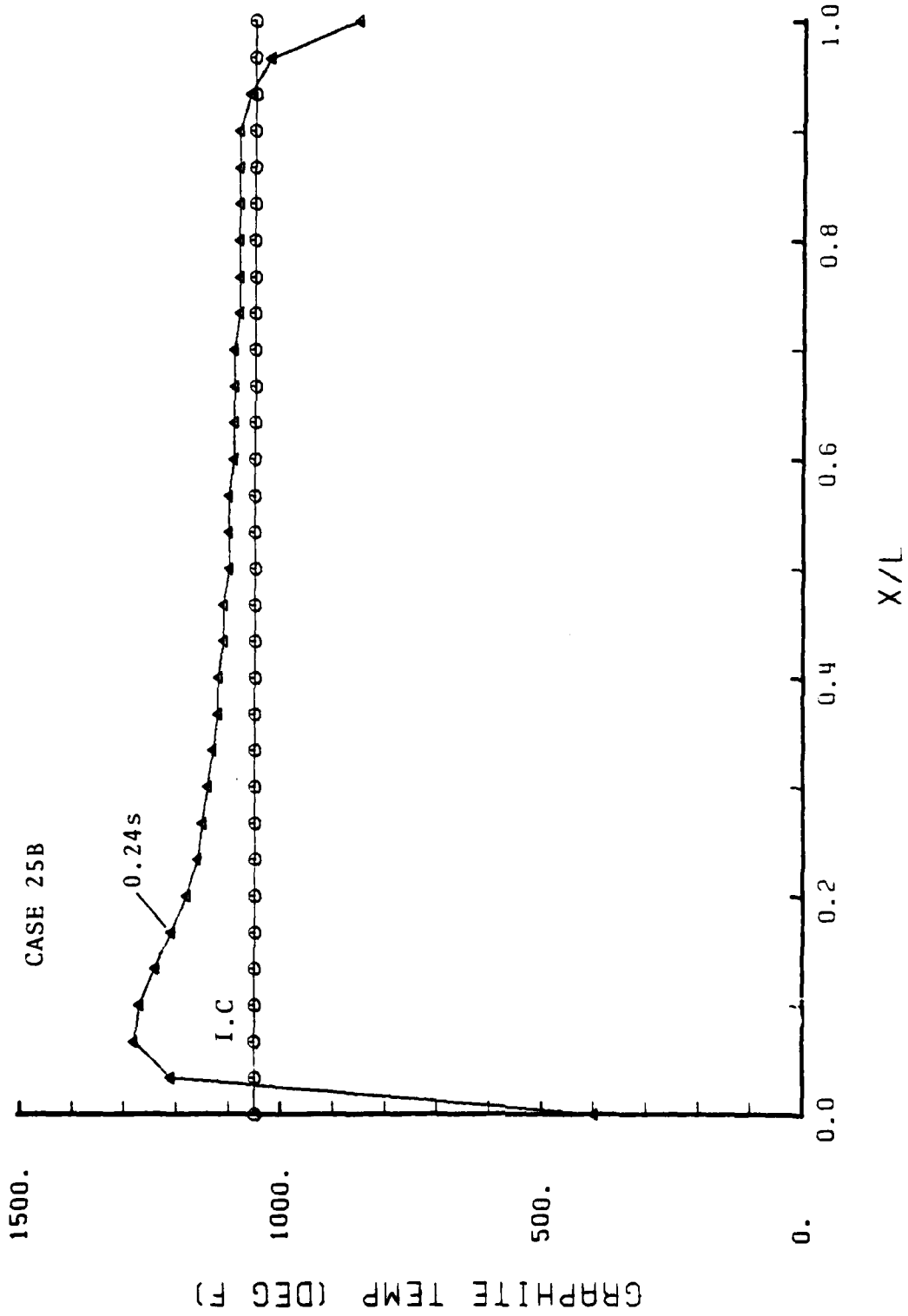


FIGURE 22. Graphite Temperature - Case 25B ($U_{\infty} = 70\text{KTS}$; $d = .0002''$; $D = .0007''$; $L = 0.5''$).

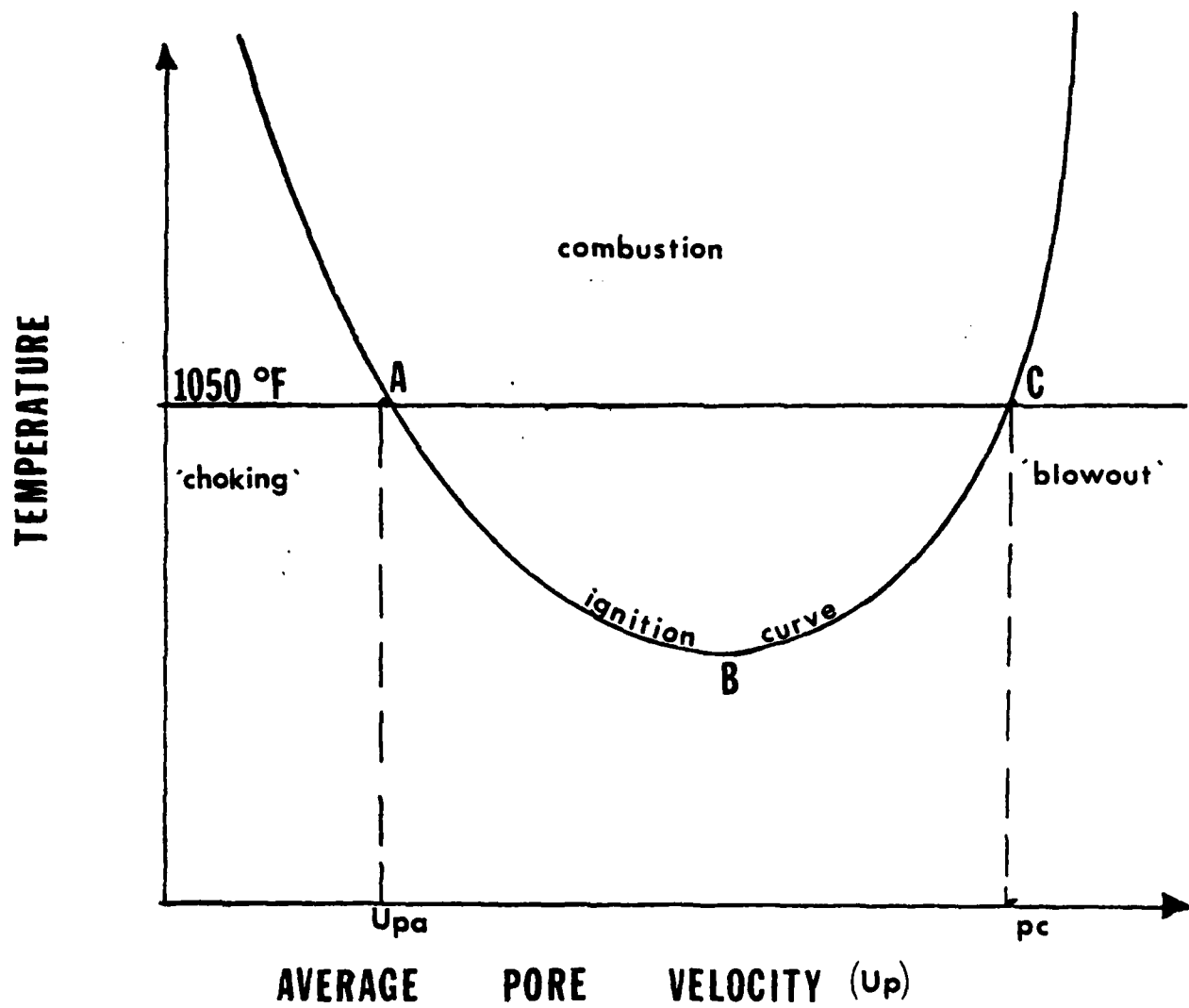


FIGURE 23. Ignition Curve for a Composite Plate

LIST OF REFERENCES

1. Jones, R.M., Mechanics of Composite Materials, Scripta Book Co., Washington, D.C., 1975.
2. Fontenot, J.S., "Graphite-Epoxy Composite Material Response to Carrier Deck Fires," Naval Weapons Center, NWC Technical Memorandum 3351, November, 1979.
3. Vatikiotis, C.S., "Analysis of Combustion and Heat Transfer in a Porous Graphite Medium," Naval Postgraduate School Thesis, June, 1980.
4. Muskat, M., The Flow of Homogeneous Fluids Through Porous Media, McGraw-Hill Book Co., New York, 1946.
5. Scheidegger, A.E., The Physics of Flow Through Porous Media, University of Toronto Press, Toronto, 1974.
6. Yoshida, F., Ramaswami, D., and Hougen, D.A., "Temperature and Partial Pressures at the Surfaces of Catalyst Particles," A.I. Ch. E. Journal, 8, 1962.
7. Frank-Kamenetskii, D.A., Diffusion and Heat Transfer in Chemical Kinetics, Plenum Press, New York, 1969.
8. Dankwerts, P.V. "Distribution of Residence Time," Chem. Eng. Sci., 2, 1, 1953.

INITIAL DISTRIBUTION LIST

	NO. Copies
1. Defense Technical Information Center Cameron Station Alexandria, Virginia 22314	2
2. Library, Code 0142 Naval Postgraduate School Monterey, California 93940	2
3. Department Chairman, Code 69 Department of Mechanical Engineering Naval Postgraduate School Monterey, California 93940	2
4. Associate Professor D. Salinas, Code 69Zc Department of Mechanical Engineering Naval Postgraduate School Monterey, California 93940	2
5. LCDR Robert E. Luby, Jr. 9021 S. Richmond Evergreen Park, Illinois 60642	3
6. Mr. John Fontenot, Code 3383 Survivability and Lethality Division Systems Development Department Naval Weapons Center China Lake, California 93555	2